

## Electronic supplementary information for

### Substituent effect on the ligand-centred electrocatalytic hydrogen evolution of antimony(III) corroles

*Qing-Hua Yu<sup>a</sup>, Yu-Fei Li<sup>b</sup>, Xu-You Cao<sup>a</sup>, Liang-Hong Liu<sup>a</sup>, Jun-Ying*

*Chen<sup>\*a</sup>, Li-Ping Si<sup>\*a, c</sup> and Hai-Yang Liu<sup>\*a</sup>*

*a. School of Chemistry and Chemical Engineering, Guangdong Provincial Key  
Laboratory of Fuel Cell Technology, South China University of Technology,  
Guangzhou 510641, P.R. China*

*b. Department of Chemistry, University College London, Christopher Ingold  
Lab, 20 Gordon Street, London WC1H 0AJ, UK*

*c. School of Materials Science and Energy Engineering, Foshan University,  
Foshan 528000, P.R. China*

*\*Corresponding Author: [chhyliu@scut.edu.cn](mailto:chhyliu@scut.edu.cn)*

## 1. General information

All reagents were purchased commercially and were used without further purification unless otherwise pointed out.  $^1\text{H}$  and  $^{19}\text{F}$  NMR spectra were recorded on a Bruker Avance III 400 MHz NMR spectrometer. The NMR spectra were referenced to the  $\text{CDCl}_3$  residual solvent signal (7.26 ppm). UV-vis spectra in  $\text{CH}_2\text{Cl}_2$  were recorded using a Hitachi U-3010 spectrophotometer at room temperature. High-resolution mass spectra (HRMS) were obtained using the Bruker microQ-TOF-QII high resolution spectrometer in the electrospray ionization (ESI) mode using Bruker Daltonics coupled to a Water Acquint system. X-ray photoelectron spectroscopy (XPS) was measured using an Axis Ultra DLD spectrophotometer, correcting the binding energies by comparing to C 1s peak (284.8 eV) by the adventitious hydrocarbon. Electrochemical measurements were performed with a CHI-660E electrochemical workstation at room temperature under saturated  $\text{N}_2$ . The three-electrode cell had glass carbon (GC) as the working electrode, graphite rod as the counter electrode, saturated  $\text{Ag}/\text{AgNO}_3$  as the reference electrode in DMF, and  $\text{Ag}/\text{AgCl}$  as the reference electrode in aqueous solutions. Ferrocene was added as an internal standard in DMF. The  $E_{1/2}$  value of reference  $\text{Fc}/\text{Fc}^+$  couple is -0.005 V in DMF. Controlled potential electrolysis (CPE) test was performed in a single electrolytic cell filled with 20 mL of buffer solution (DMF:  $\text{H}_2\text{O}$  1:2) with 0.1 M KCl and 0.25 M  $\text{KH}_2\text{PO}_4$ .

## 2. Synthesis methods

5,10,15-tris (pentafluorophenyl) corrole ( $\text{F}_{15}\text{C}$ ), 5,15-bis (pentafluorophenyl)-10-(phen-yl) corrole ( $\text{F}_{10}\text{C}$ ), 5,15-bis (phenyl)-10-(pentafluorophenyl) corrole ( $\text{F}_5\text{C}$ ), 5,10,15-tris (phe-nyl) corrole ( $\text{F}_0\text{C}$ ), 5,10,15-tris (pentafluorophenyl) Sb(III) corrole ( $\text{F}_{15}\text{C-Sb}$ ) and 5,10,15-tris (phenyl) corrole Sb(III) ( $\text{F}_0\text{C-Sb}$ ) were prepared by previously published procedures.<sup>1-3</sup>

### 5,10,15-tris (pentafluorophenyl) corrole ( $\text{F}_{15}\text{C}$ )

$^1\text{H}$  NMR (400 MHz, Chloroform-*d*)  $\delta$  9.12 (d,  $J = 4.3$  Hz, 2H), 8.77 (d,  $J = 4.7$  Hz, 2H), 8.58 (t,  $J = 5.3$  Hz, 4H).  $^{19}\text{F}$  NMR (376 MHz, Chloroform-*d*)  $\delta$  -137.18 (s,2F), -137.72 (s,4F), -152.10 (s,2F), -152.69 (s,1F), -161.34 (s,4F), -161.82 (s,2F). HRMS-ESI:  $m/z$  calcd. for  $[\text{C}_{37}\text{H}_{11}\text{F}_{15}\text{N}_4+\text{H}^+]$ : 797.0817  $[\text{M}+\text{H}]^+$ ; found: 797.0815.

### 5,15-bis (pentafluorophenyl)-10-(phenyl) corrole ( $\text{F}_{10}\text{C}$ )

$^1\text{H}$  NMR (400 MHz, Chloroform-*d*)  $\delta$  9.10 (s, 2H), 8.72 (s, 4H), 8.55 (s, 2H), 8.18 (s, 2H), 7.82 – 7.73 (m, 3H).  $^{19}\text{F}$  NMR (376 MHz, Chloroform-*d*)  $\delta$  -137.86 (s, 4F), -152.86 (s, 2F), -161.78 (s, 4F). HRMS-ESI:  $m/z$  calcd. for  $[\text{C}_{37}\text{H}_{16}\text{F}_{10}\text{N}_4+\text{H}^+]$ : 707.1288  $[\text{M}+\text{H}]^+$ ; found: 707.1284.

### 5,15-bis (phenyl)-10-(pentafluorophenyl) corrole ( $F_5C$ )

$^1H$  NMR (400 MHz, Chloroform-*d*)  $\delta$  8.92 (s, 4H), 8.55 (s, 2H), 8.43 (s, 2H), 8.34 (d,  $J = 7.4$  Hz, 4H), 7.81 (d,  $J = 7.9$  Hz, 4H), 7.74 (d,  $J = 7.6$  Hz, 2H).  $^{19}F$  NMR (376 MHz, Chloroform-*d*)  $\delta$  -137.43 (d,  $J = 24.8$  Hz, 2F), -153.90 (t,  $J = 20.9$  Hz, 1F), -162.44 (t,  $J = 20.8$  Hz, 2F). HRMS-ESI:  $m/z$  calcd. for  $[C_{37}H_{21}F_5N_4+H]^+$ : 617.1759  $[M+H]^+$ ; found: 617.1752.

### 5,10,15-tris (phenyl) corrole ( $F_0C$ )

$^1H$  NMR (400 MHz, Chloroform-*d*)  $\delta$  9.02 – 8.66 (m, 4H), 8.42 (d,  $J = 62.1$  Hz, 8H), 8.14 (s, 2H), 7.76 (d,  $J = 7.1$  Hz, 9H). HRMS-ESI:  $m/z$  calcd. for  $[C_{37}H_{26}N_4+H]^+$ : 527.2230  $[M+H]^+$ ; found: 527.2232.

### 5,10,15-tris (pentafluorophenyl) Sb(III) corrole ( $F_{15}C-Sb$ )

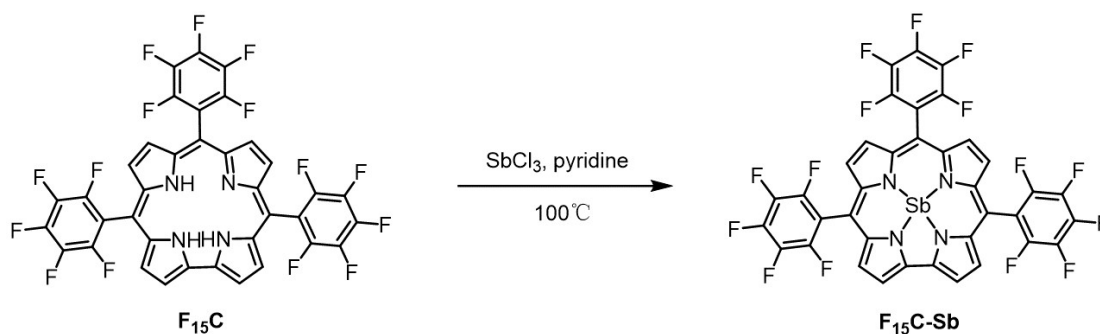


Fig. S1 Synthetic routes of Sb(III) corrole

The specific synthesis steps of Sb(III) corrole are exemplified by  $F_{15}C-Sb$ . Dissolve 100 mg  $F_{15}C$  (0.13 mmol) and 480 mg  $SbCl_3$  (2.02 mmol) in a round-bottomed flask with 10 ml pyridine. Then the temperature was raised to  $100^\circ C$  and reacted for 2 hours, and the solution turned into dark green. Remove excess solvent with a rotary evaporator, and fill the column with 100 ~ 200 mesh silica gel. Use dichloromethane and hexane (DCM/Hex) (V/V) = 3/1 as an eluent to purify the product. After recrystallization obtain green solid (96.26 mg, yield 83.50%).  $^1H$  NMR (400 MHz, Chloroform-*d*)  $\delta$  9.25 (d,  $J = 4.2$  Hz, 2H), 8.90 (dd,  $J = 4.7, 1.4$  Hz, 2H), 8.72 (d,  $J = 4.2$  Hz, 2H), 8.65 (d,  $J = 4.6$  Hz, 2H).  $^{19}F$  NMR (376 MHz, Chloroform-*d*)  $\delta$  -136.75 (dd,  $J = 24.9, 7.1$  Hz, 2F), -136.99 (ddd,  $J = 74.3, 24.9, 8.6$  Hz, 2F), -137.32 (dd,  $J = 24.3, 8.3$  Hz, 2F), -152.31 (t,  $J = 21.0$  Hz, 2F), -152.64 (t,  $J = 20.9$  Hz, 1F), -161.31 to -162.07 (m, 6F). HRMS-ESI:  $m/z$  calcd. for  $[C_{37}H_{11}F_{15}N_4+H]^+$ : 914.9620  $[M+H]^+$ ; found: 914.9623.

### 5,15-bis (pentafluorophenyl)-10-(phenyl) Sb(III) corrole ( $F_{10}C-Sb$ )

The synthetic route was similar to  $F_{15}C-Sb$ , after recrystallization obtain pure antimony corrole (green solid, yield 86.52%).  $^1H$  NMR (400 MHz, Chloroform-*d*)  $\delta$  9.32 (d,  $J = 4.2$  Hz,

2H), 8.91 (dd,  $J = 4.7, 1.5$  Hz, 2H), 8.87 (d,  $J = 4.6$  Hz, 2H), 8.78 (dd,  $J = 4.2, 1.3$  Hz, 2H), 8.35 (s, 1H), 7.97 (s, 1H), 7.83 – 7.70 (m, 3H).  $^{19}\text{F}$  NMR (376 MHz, Chloroform-*d*)  $\delta$  -136.87 (ddd,  $J = 24.6, 8.2, 3.0$  Hz, 2F), -137.46 (ddd,  $J = 23.9, 8.5, 3.0$  Hz, 2F), -152.93 (t,  $J = 21.0$  Hz, 2F), -161.87 (dddd,  $J = 57.6, 24.5, 20.8, 8.5$  Hz, 4F). HRMS-ESI:  $m/z$  calcd. for  $[\text{C}_{37}\text{H}_{16}\text{F}_{10}\text{N}_4+\text{H}^+]$ : 824.0013  $[\text{M}+\text{H}]^+$ ; found: 824.0005.

### 5,15-bis (phenyl)-10-(pentafluorophenyl) Sb(III) corrole ( $\text{F}_5\text{C-Sb}$ )

The synthetic route was similar to  $\text{F}_{15}\text{C-Sb}$ , after recrystallization obtain pure antimony corrole (green solid, yield 76.53%).  $^1\text{H}$  NMR (400 MHz, Chloroform-*d*)  $\delta$  9.15 (dd,  $J = 10.8, 4.3$  Hz, 4H), 8.77 (d,  $J = 4.2$  Hz, 2H), 8.56 (d,  $J = 4.6$  Hz, 2H), 8.24 (s, 4H), 7.83 – 7.75 (m, 6H).  $^{19}\text{F}$  NMR (376 MHz, Chloroform-*d*)  $\delta$  -137.22 (ddd,  $J = 73.5, 24.8, 8.8$  Hz, 2F), -153.84 (t,  $J = 21.1$  Hz, 1F), -162.29 (dddd,  $J = 33.8, 21.3, 14.5, 8.4$  Hz, 2F). HRMS-ESI:  $m/z$  calcd. for  $[\text{C}_{37}\text{H}_{21}\text{F}_5\text{N}_4+\text{H}^+]$ : 734.0484  $[\text{M}+\text{H}]^+$ ; found: 734.0486.

### 5,10,15-tris (phenyl) Sb(III) corrole ( $\text{F}_0\text{C-Sb}$ )

The synthetic route was similar to  $\text{F}_{15}\text{C-Sb}$ , after recrystallization obtain pure antimony corrole (green solid, yield 80.13%).  $^1\text{H}$  NMR (400 MHz, Chloroform-*d*)  $\delta$  9.16 (dd,  $J = 28.5, 4.4$  Hz, 4H), 8.78 (dd,  $J = 16.1, 4.4$  Hz, 4H), 8.40 – 8.21 (m, 6H), 7.85 – 7.72 (m, 9H). HRMS-ESI:  $m/z$  calcd. for  $[\text{C}_{37}\text{H}_{26}\text{N}_4+\text{H}^+]$ : 644.0955  $[\text{M}+\text{H}]^+$ ; found: 644.0957.

### References:

- 1 S. Mondal, A. Garai, P. K. Naik, J. K. Adha and S. Kar, *Inorg. Chim. Acta.*, 2020, **501**, 119300.
- 2 L. Huang, A. Ali, H. Wang, F. Cheng and H. Liu, *J. Mol. Catal. A Chem.*, 2017, **426**, 213-222.
- 3 I. Luobeznova, M. Raizman, I. Goldberg and Z. Gross, *Inorg. Chem.*, 2006, **45**, 386-394.

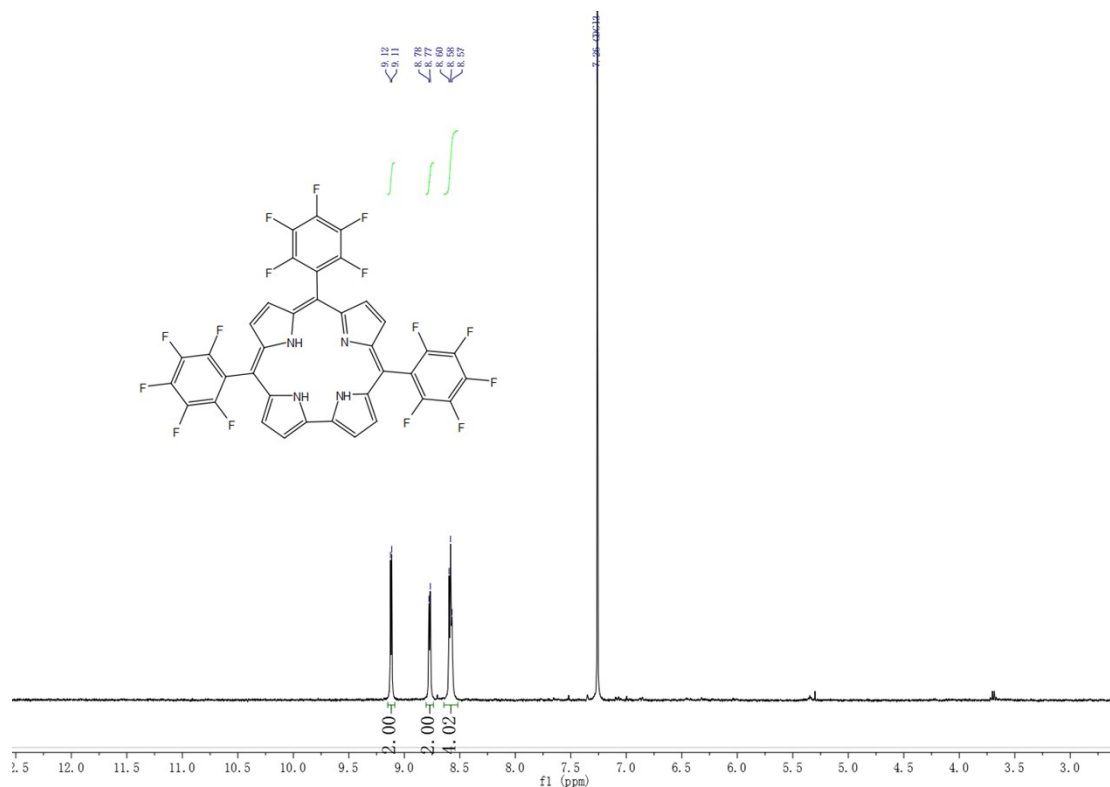


Fig. S2 <sup>1</sup>H NMR spectrum of **F<sub>15</sub>C**

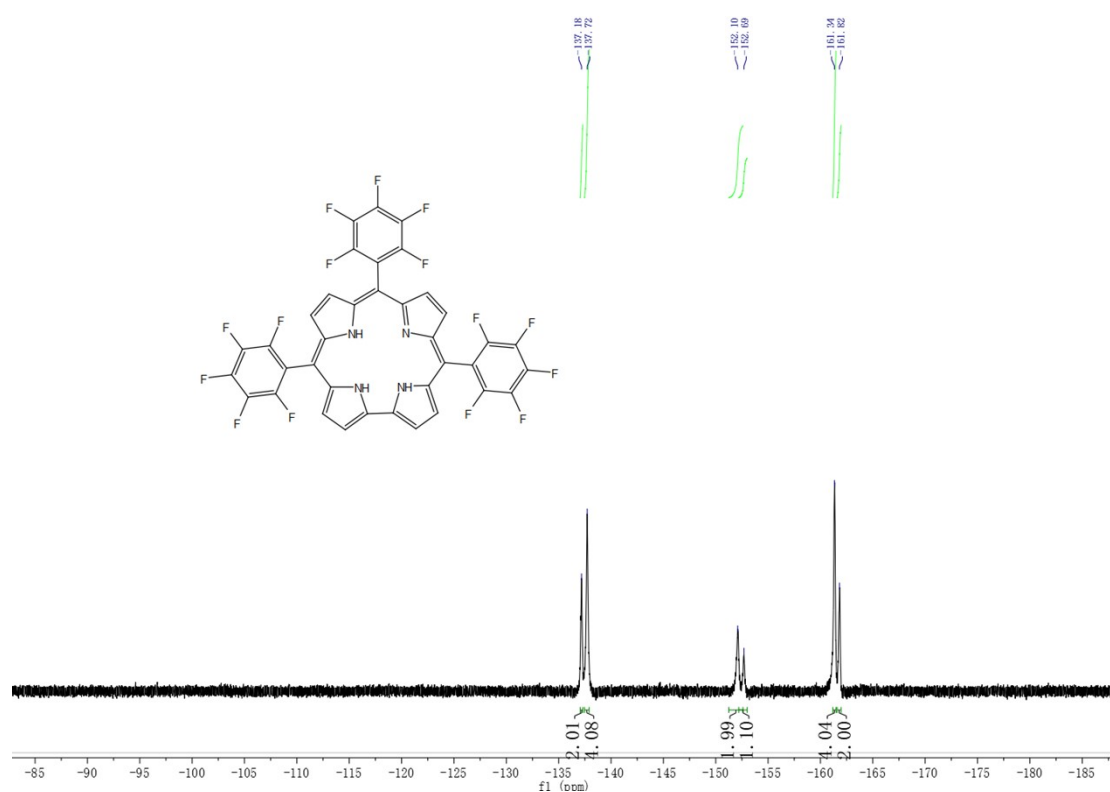


Fig. S3 <sup>19</sup>F NMR spectrum of **F<sub>15</sub>C**

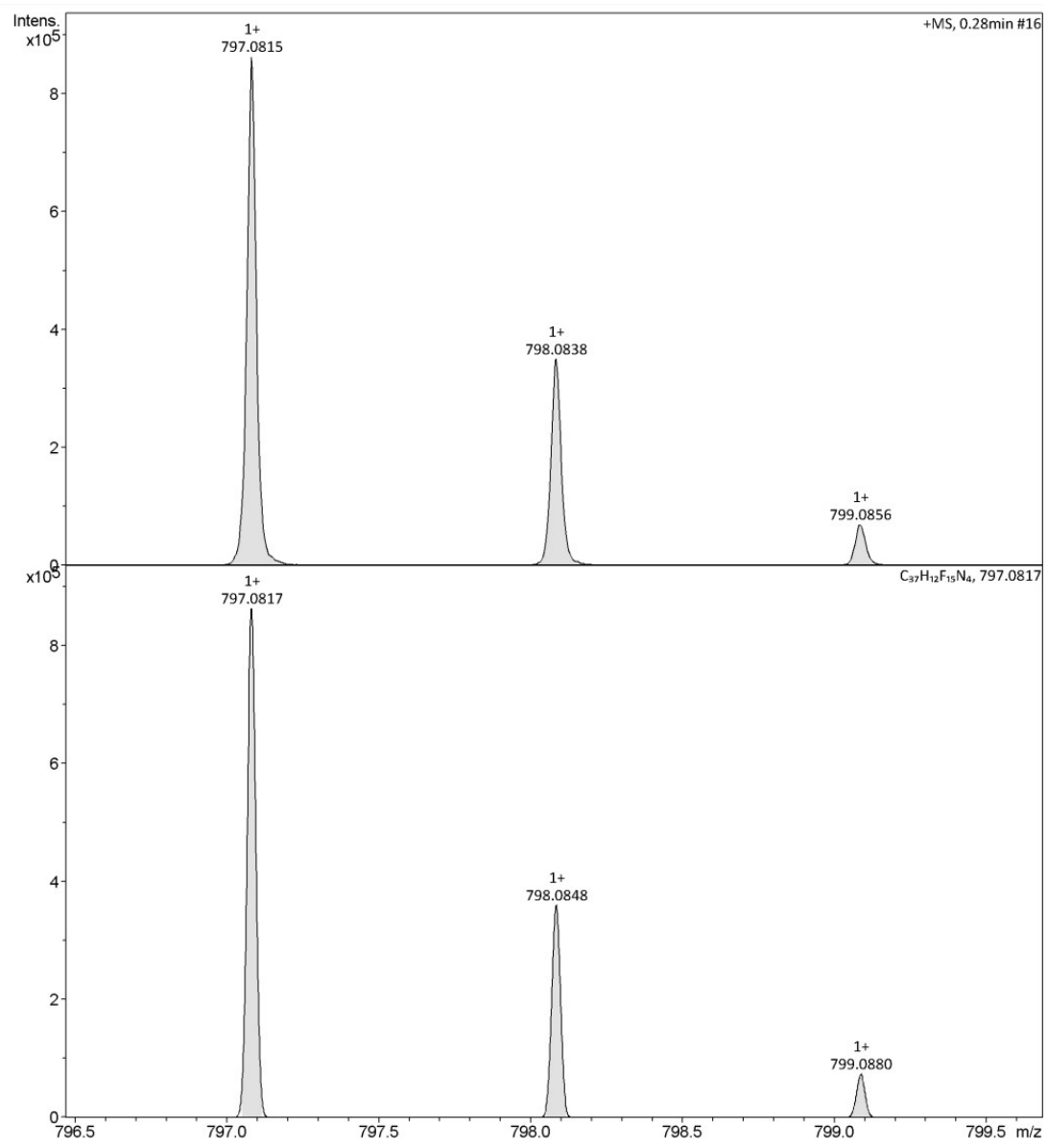


Fig. S4 ESI-HRMS spectrum of  $F_{15}C$

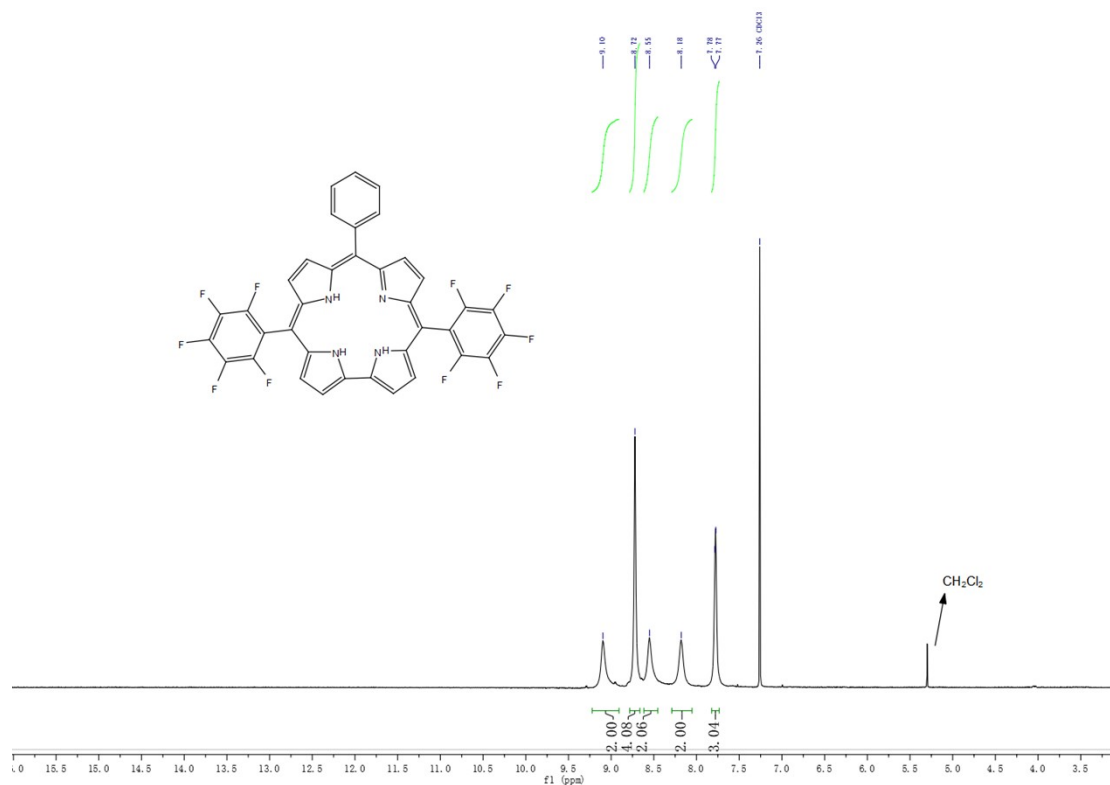


Fig. S5 <sup>1</sup>H NMR spectrum of **F<sub>10</sub>C**

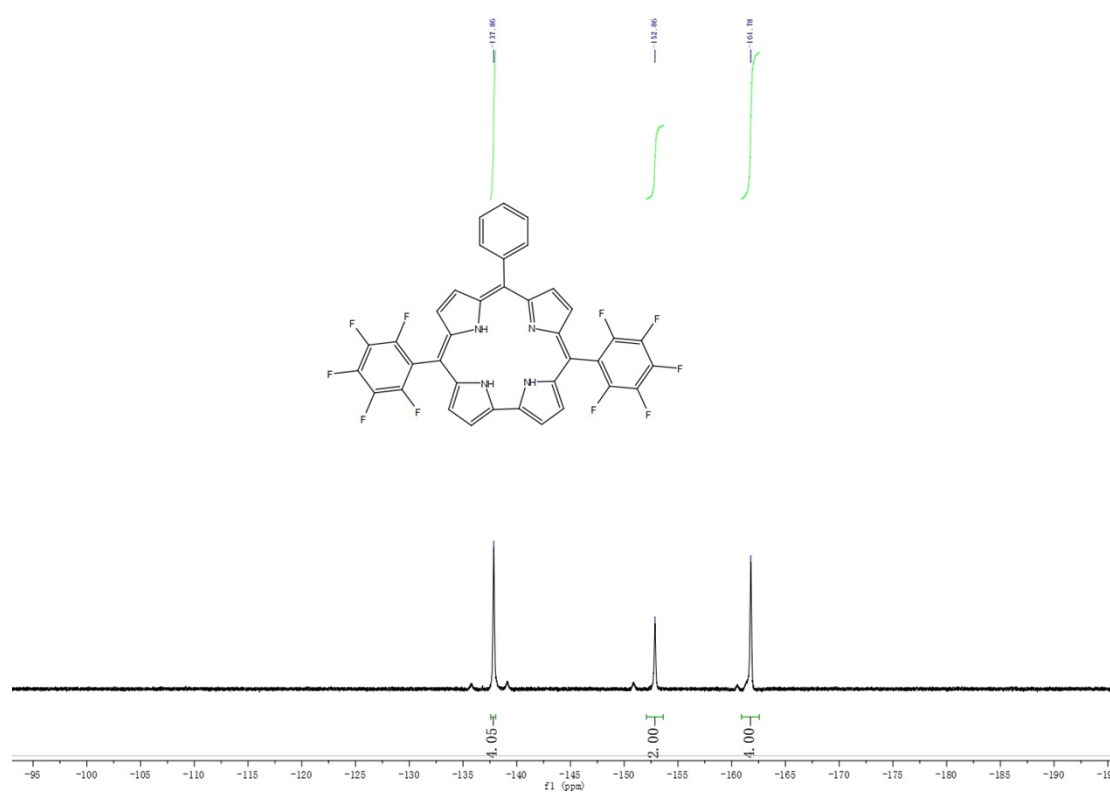


Fig. S6 <sup>19</sup>F NMR spectrum of **F<sub>10</sub>C**

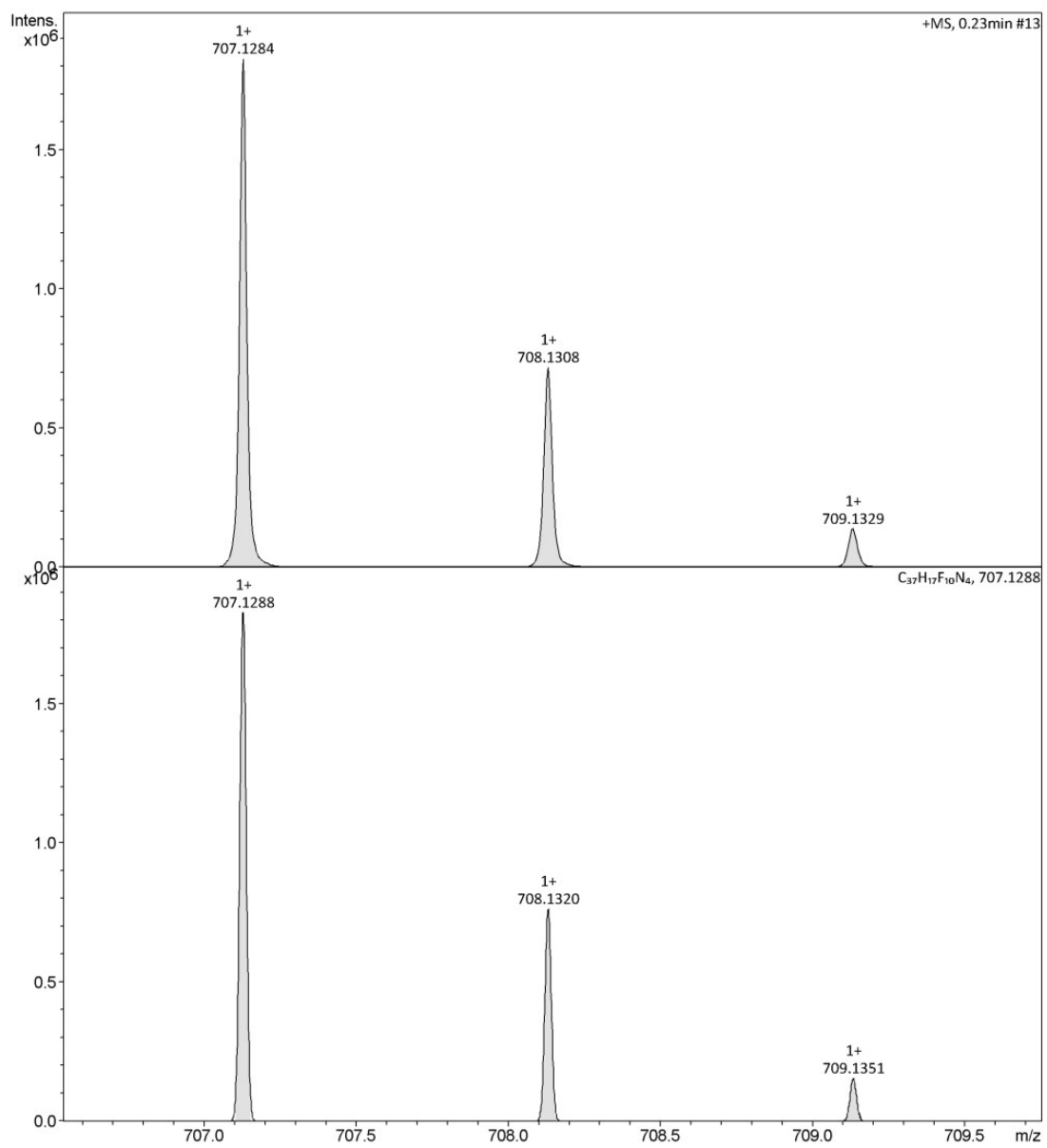


Fig. S7 ESI-HRMS spectrum of  $F_{10}C$



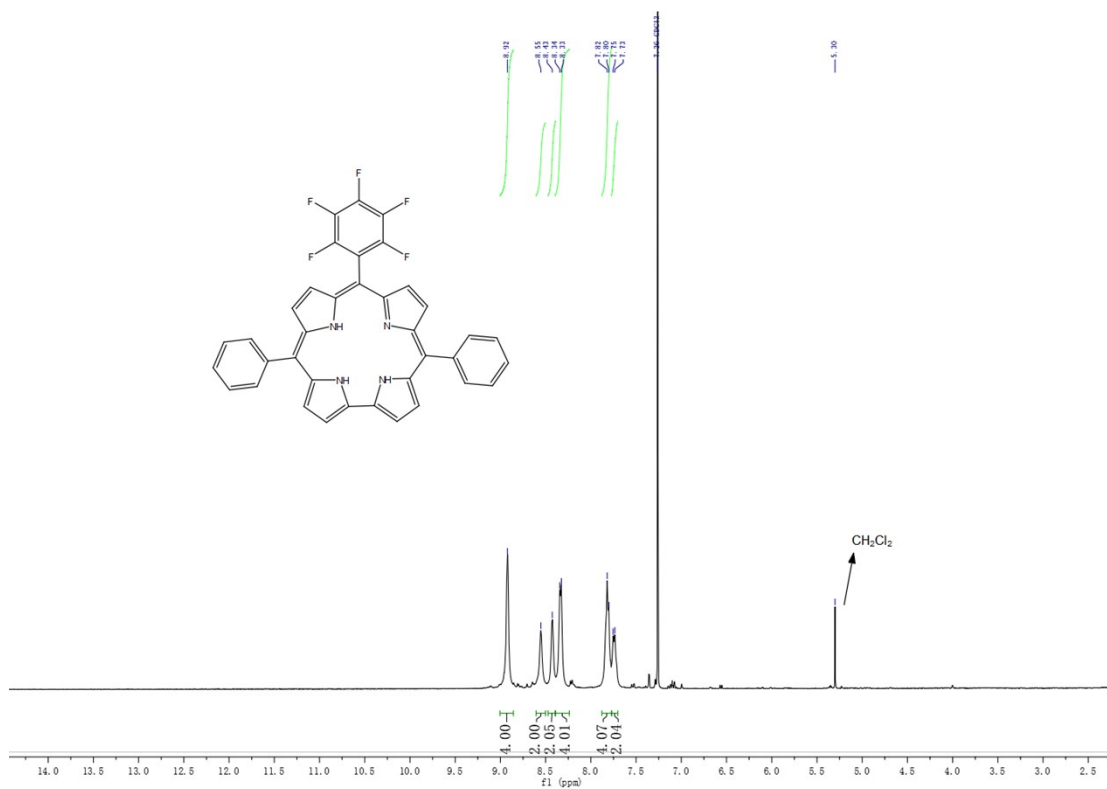


Fig. S8  $^1H$  NMR spectrum of  $F_5C$

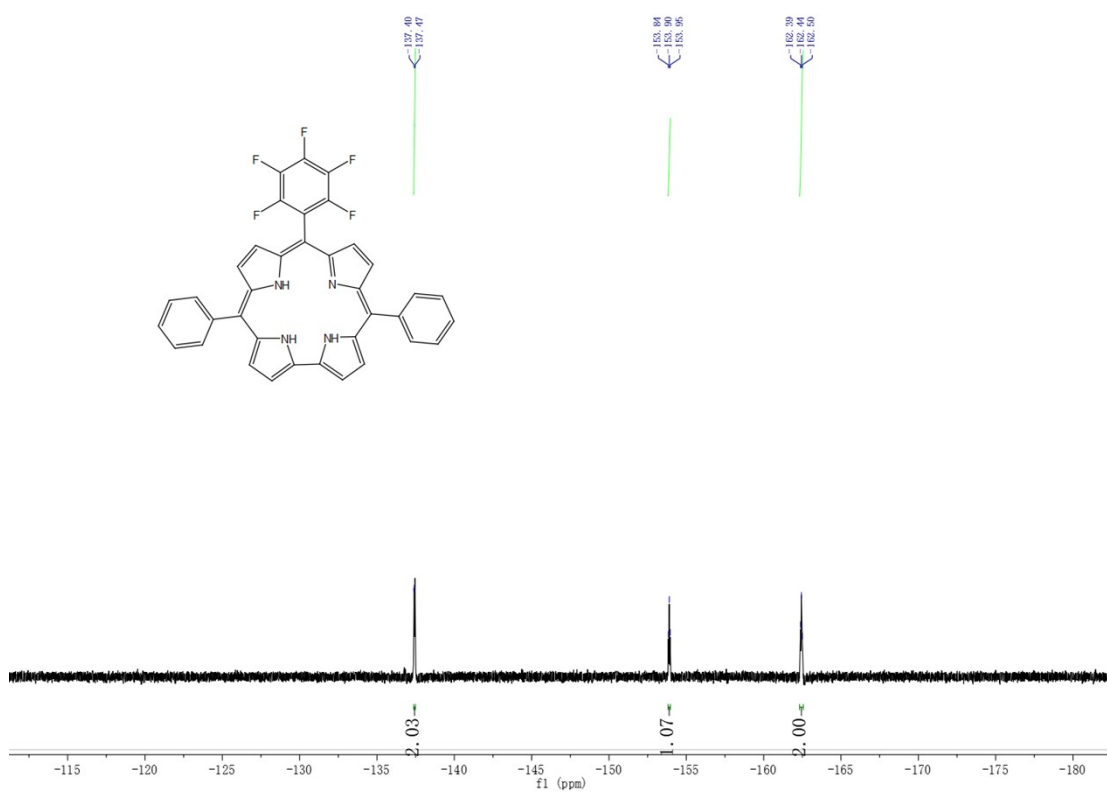


Fig. S9  $^{19}F$  NMR spectrum of  $F_5C$

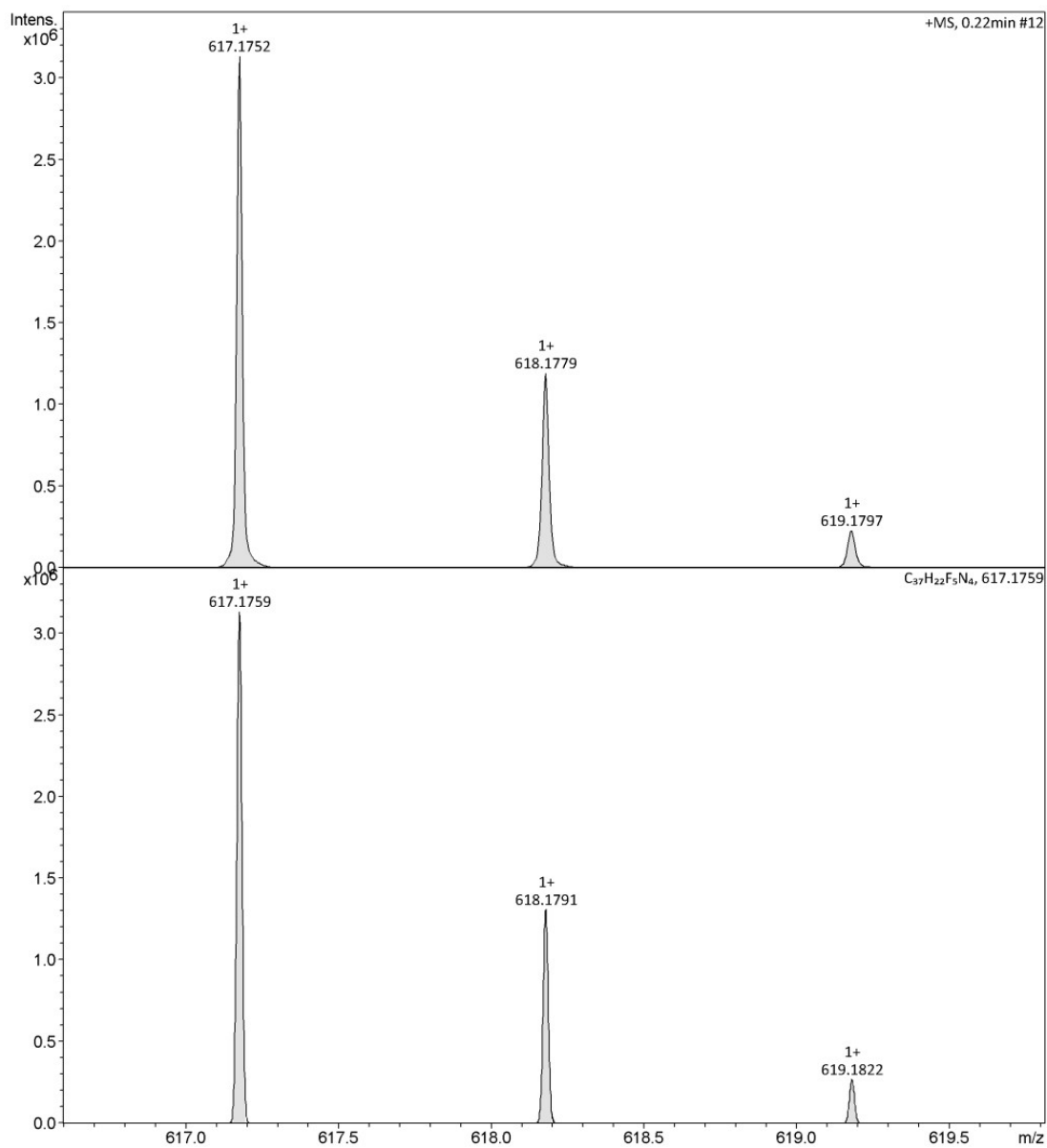


Fig. S10 ESI-HRMS spectrum of  $F_5C$

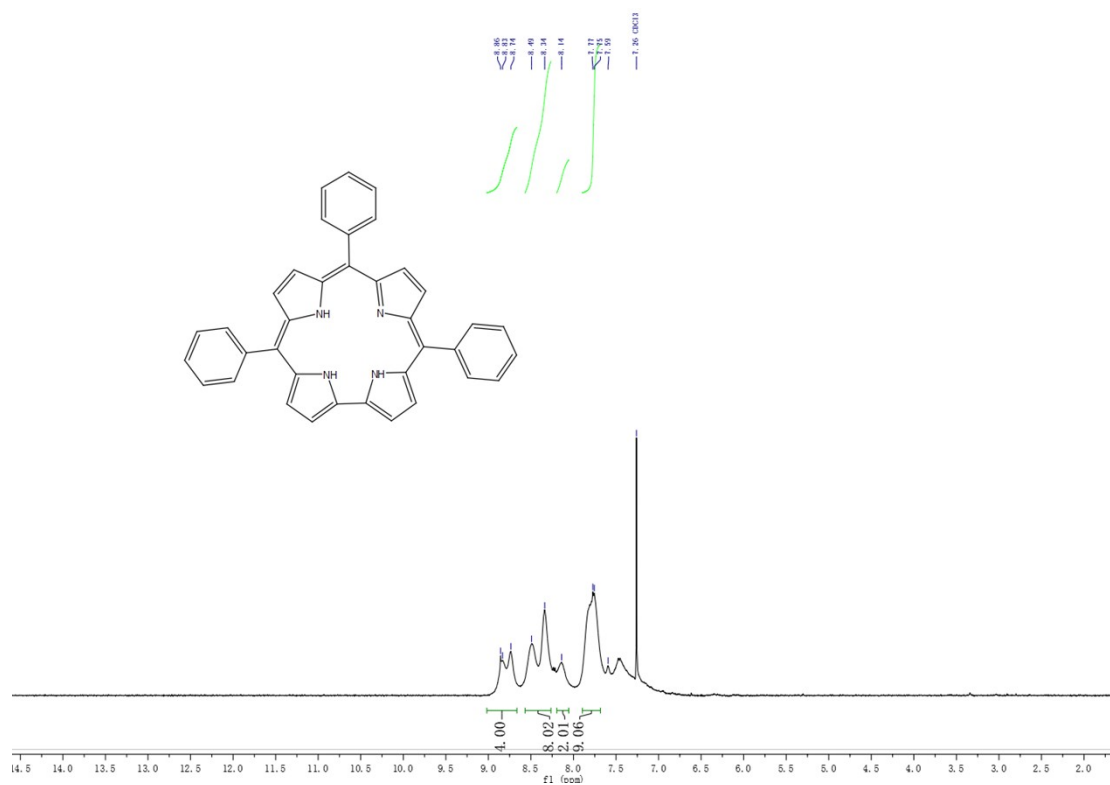


Fig. S11 <sup>1</sup>H NMR spectrum of **F<sub>0</sub>C**

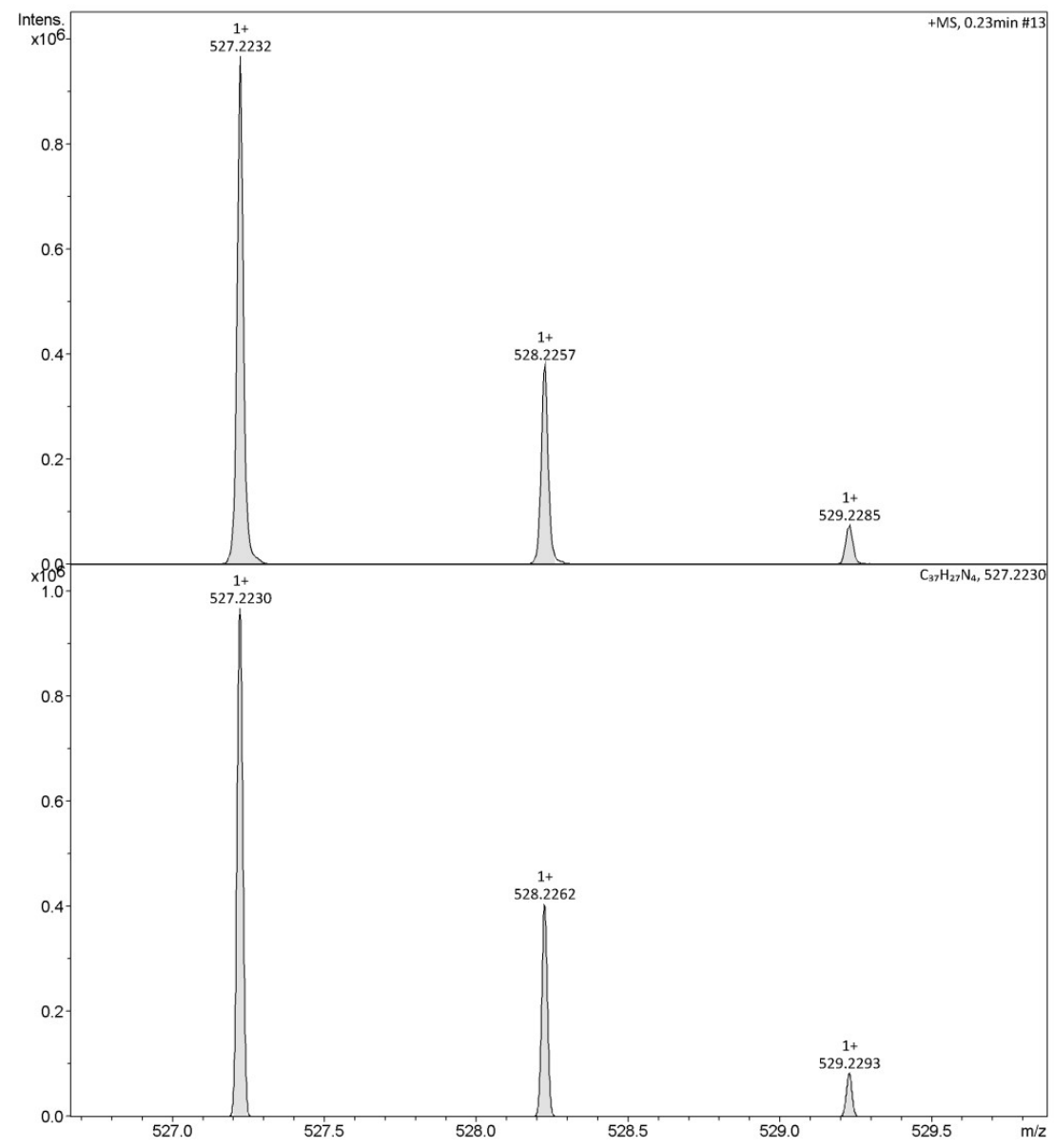


Fig. S12 ESI-HRMS spectrum of F<sub>0</sub>C

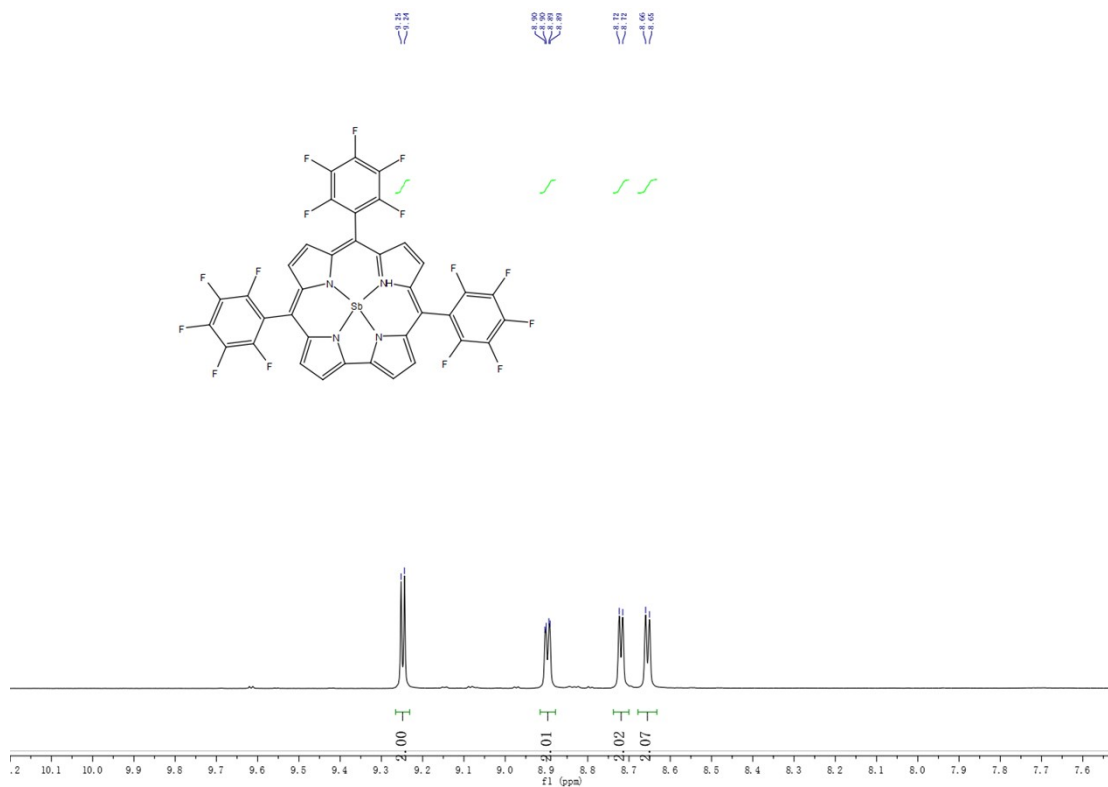


Fig. S13  $^1H$  NMR spectrum of  $F_{15}C-Sb$

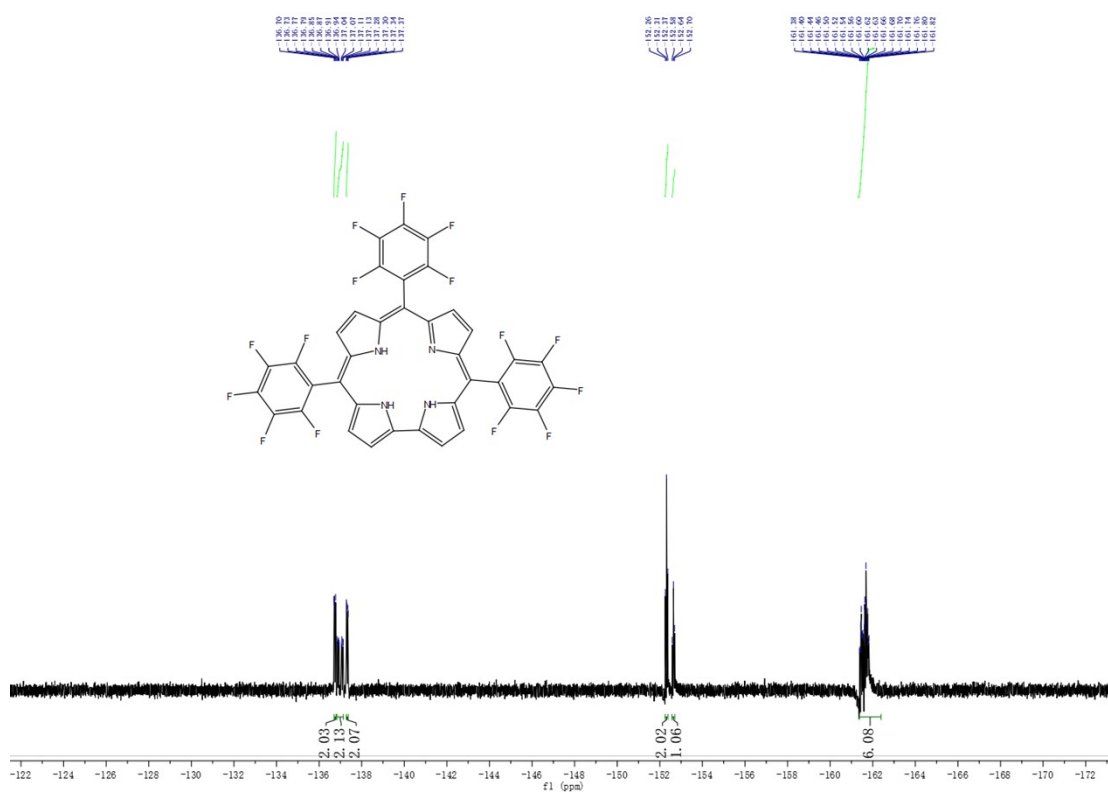


Fig. S14  $^{19}F$  NMR spectrum of  $F_{15}C-Sb$

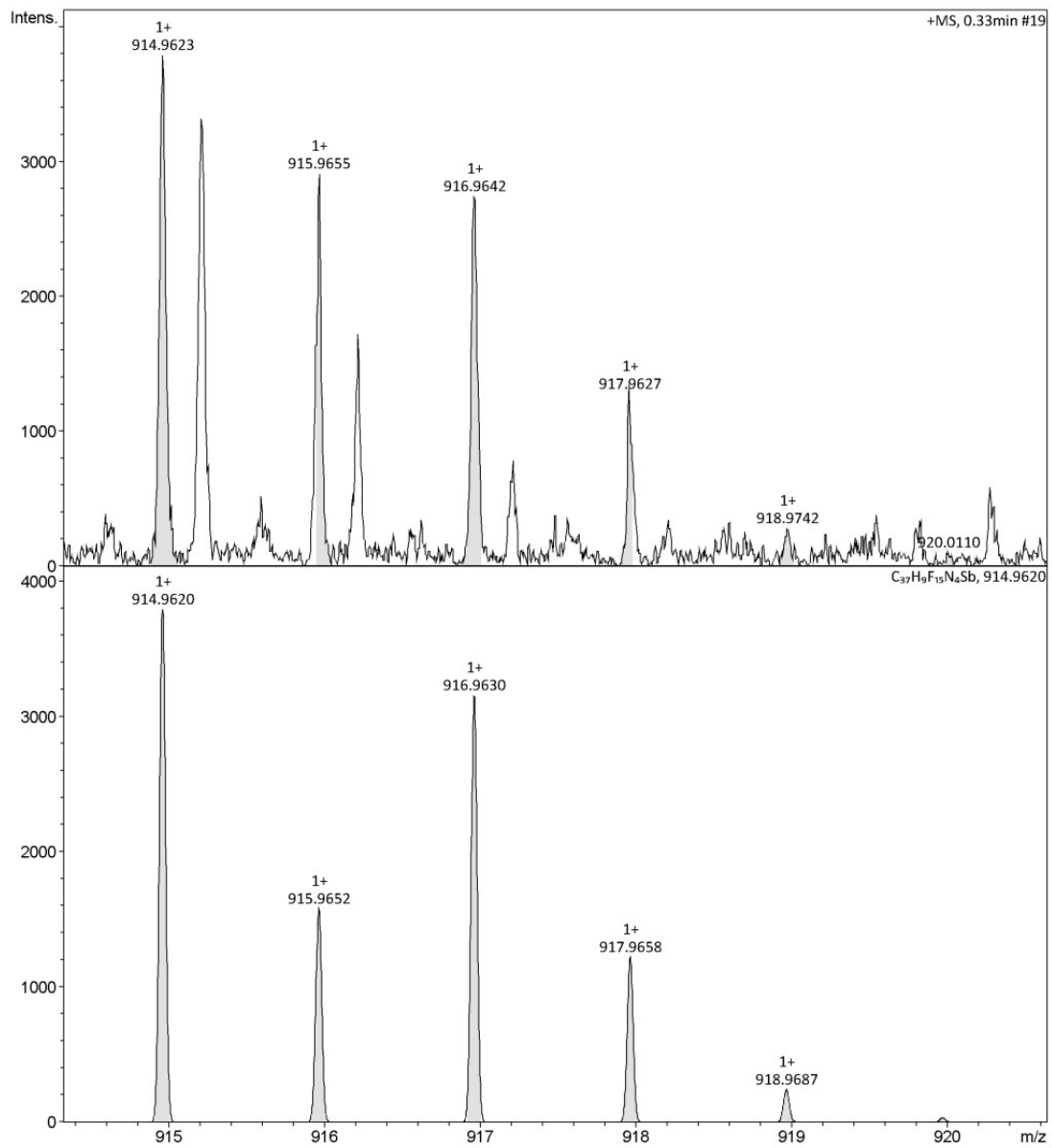


Fig. S15 ESI-HRMS spectrum of  $F_{15}C-Sb$

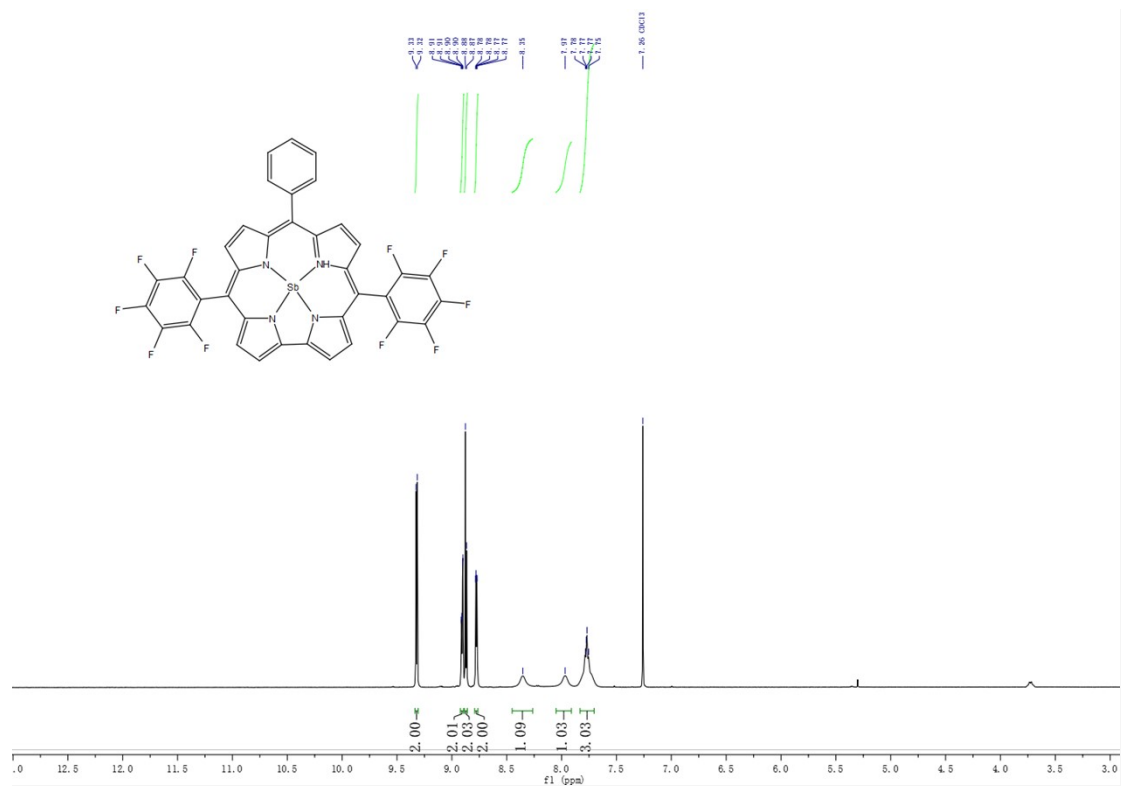


Fig. S16  $^1H$  NMR spectrum of  $F_{10}C-Sb$

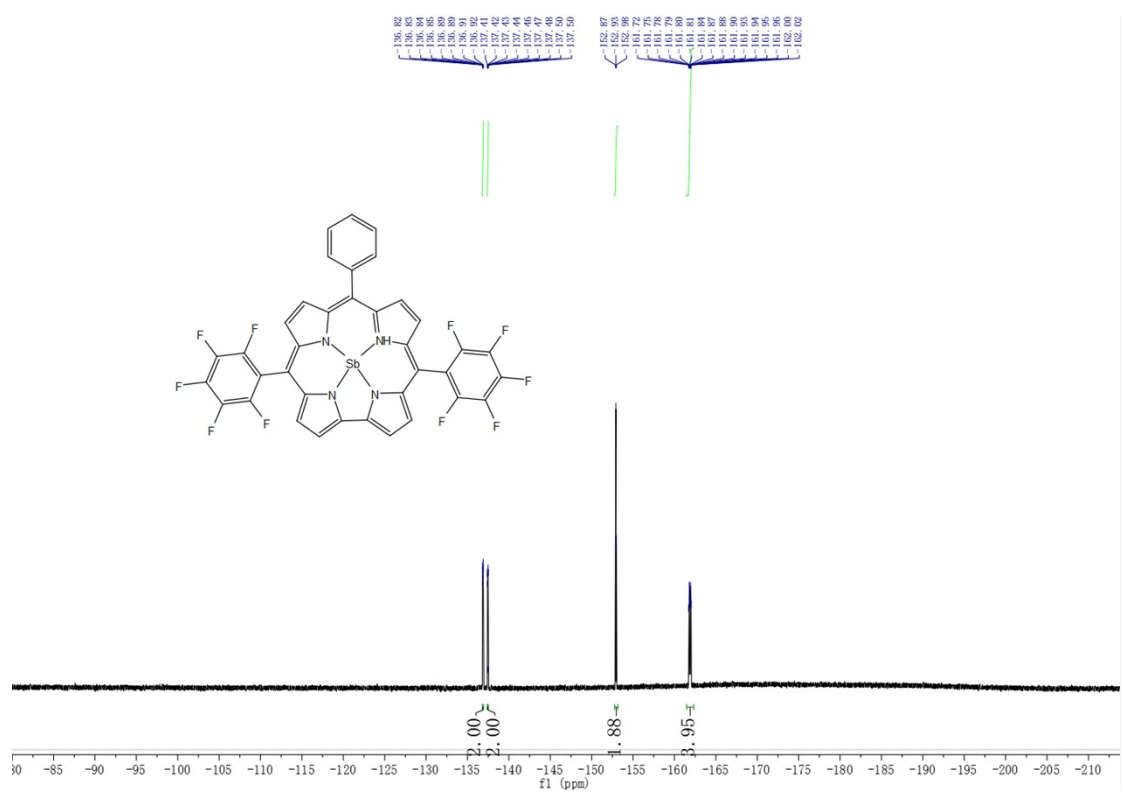


Fig. S17  $^{19}F$  NMR spectrum of  $F_{10}C-Sb$

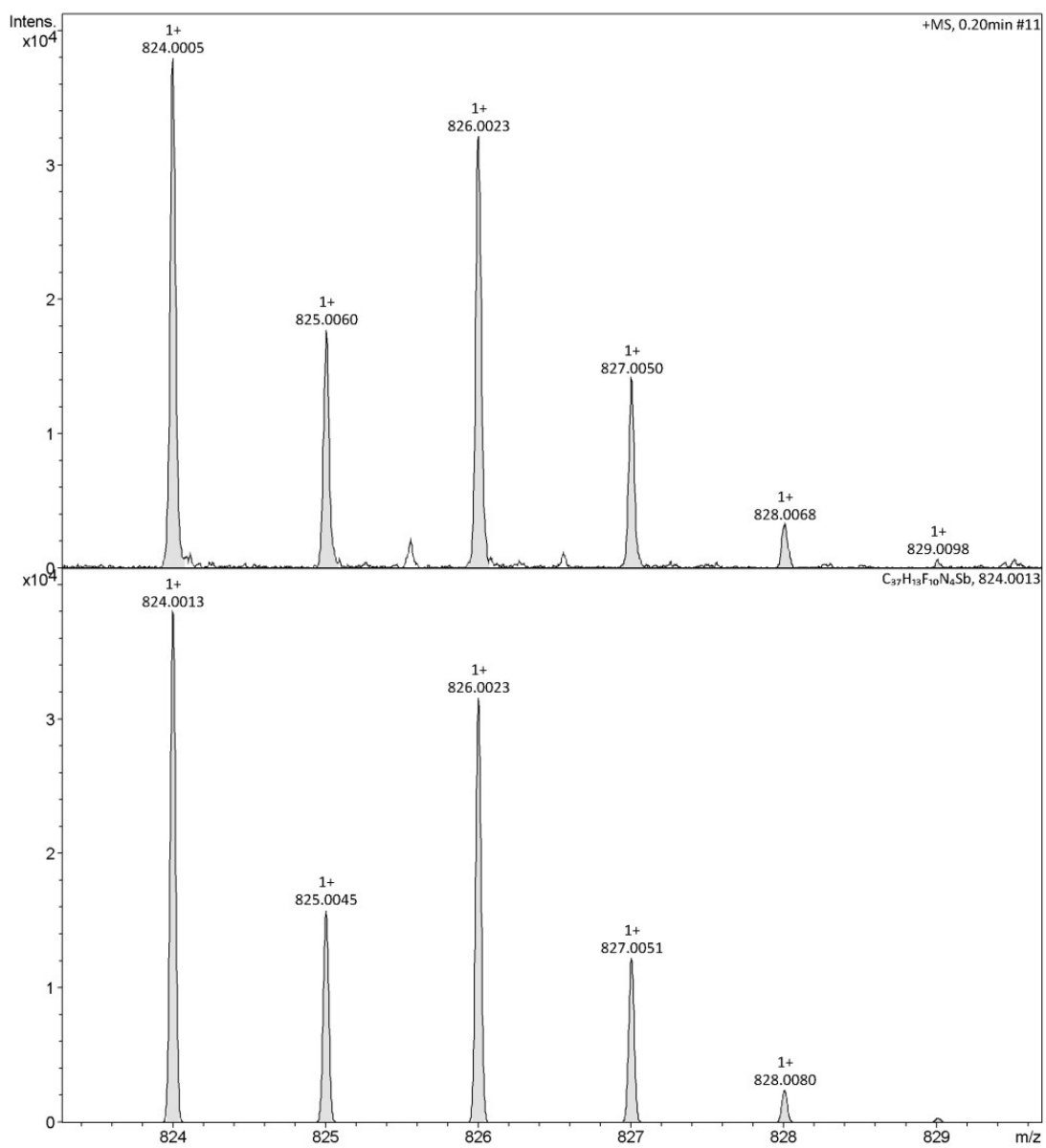


Fig. S18 ESI-HRMS spectrum of  $F_{10}C-Sb$



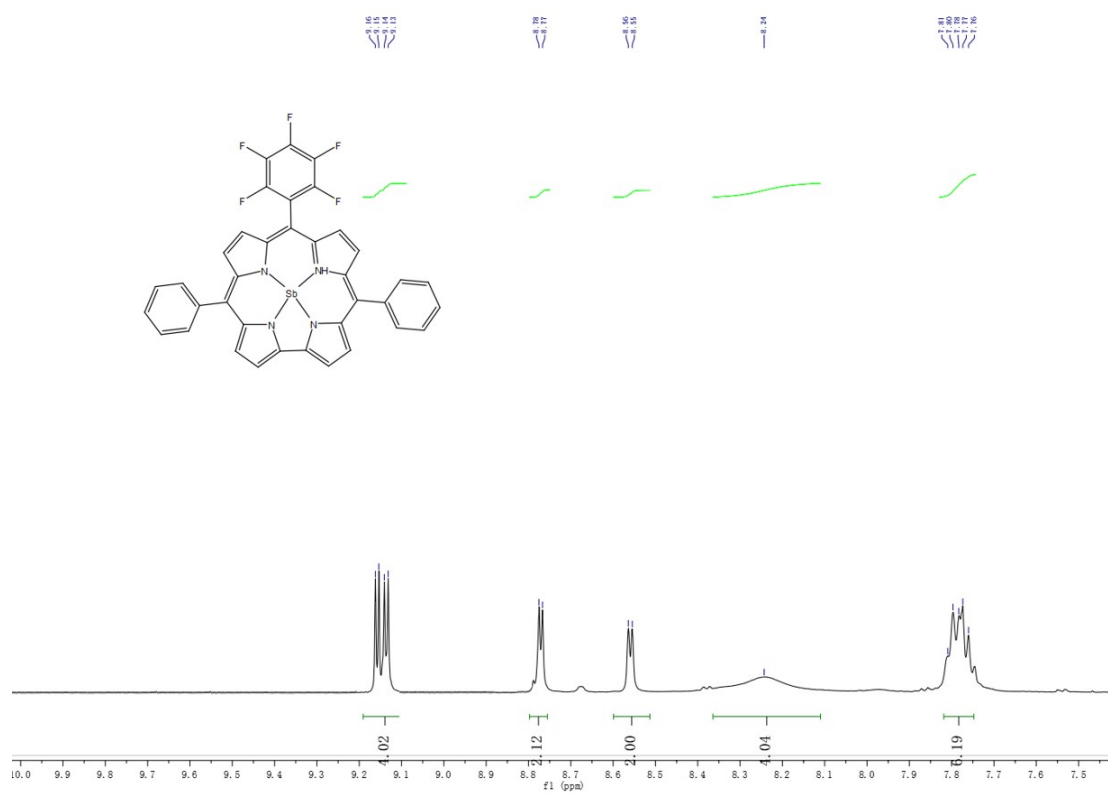


Fig. S19  $^1H$  NMR spectrum of  $F_5C-Sb$

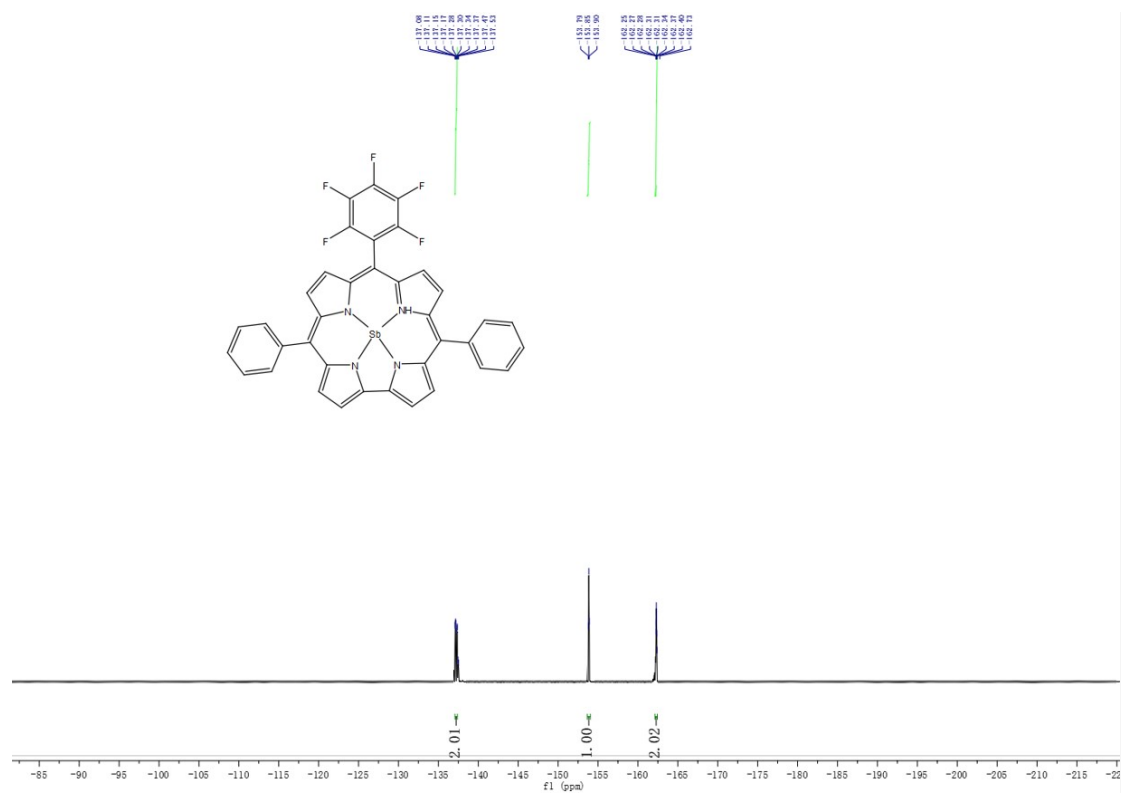


Fig. S20  $^{19}F$  NMR spectrum of  $F_5C-Sb$

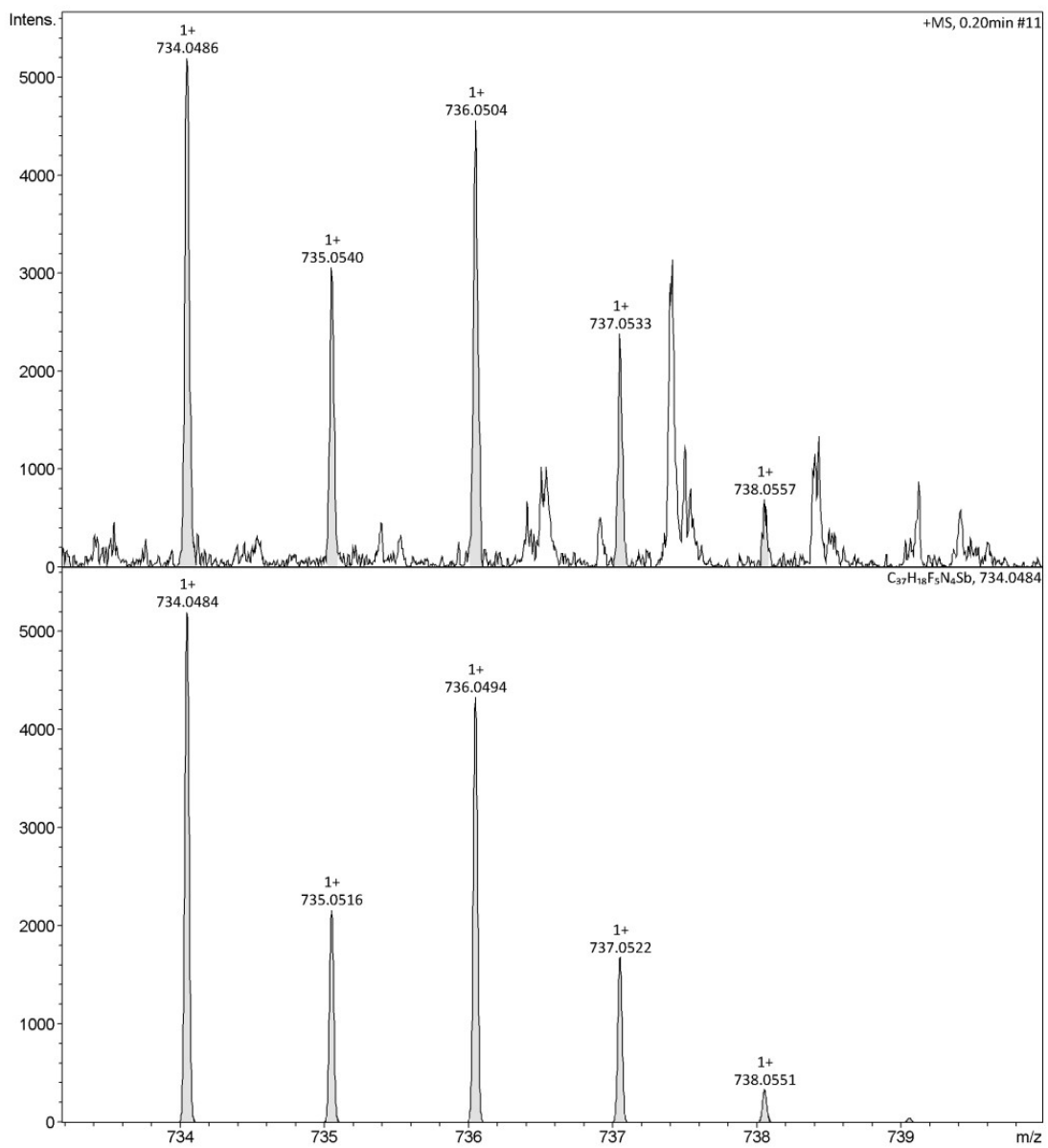


Fig. S21 ESI-HRMS spectrum of  $F_5C-Sb$

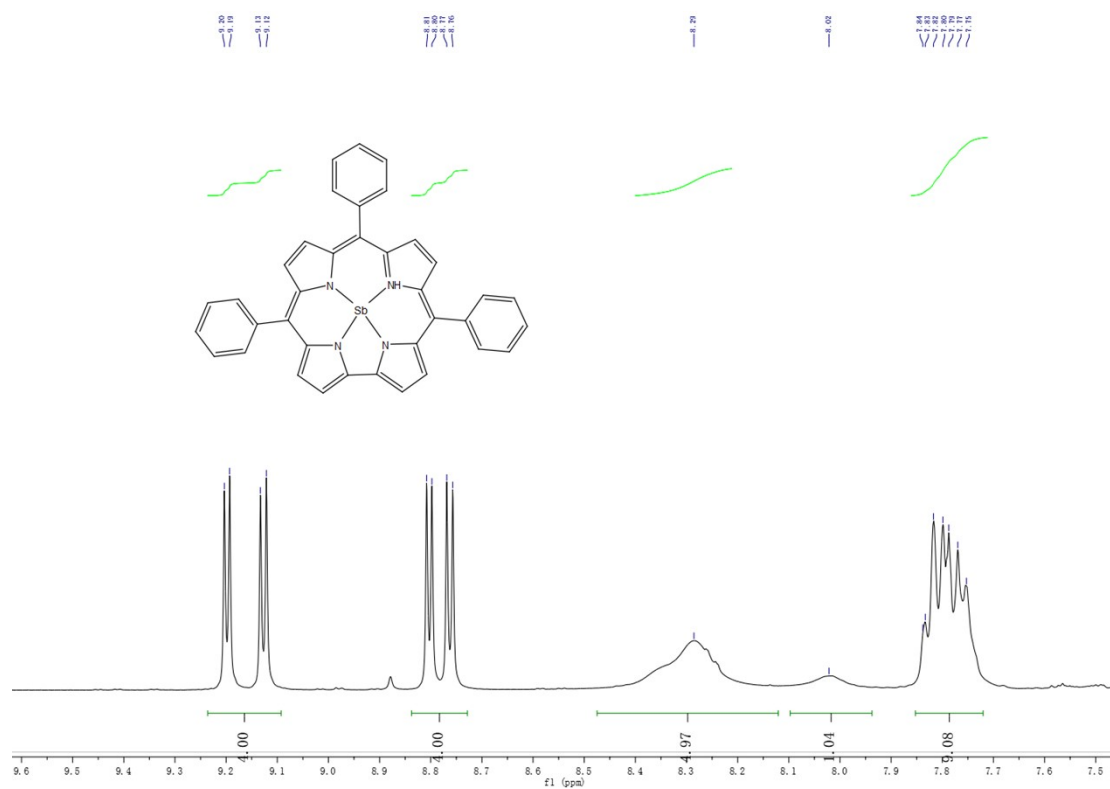


Fig. S22 <sup>1</sup>H NMR spectrum of F<sub>0</sub>C-Sb

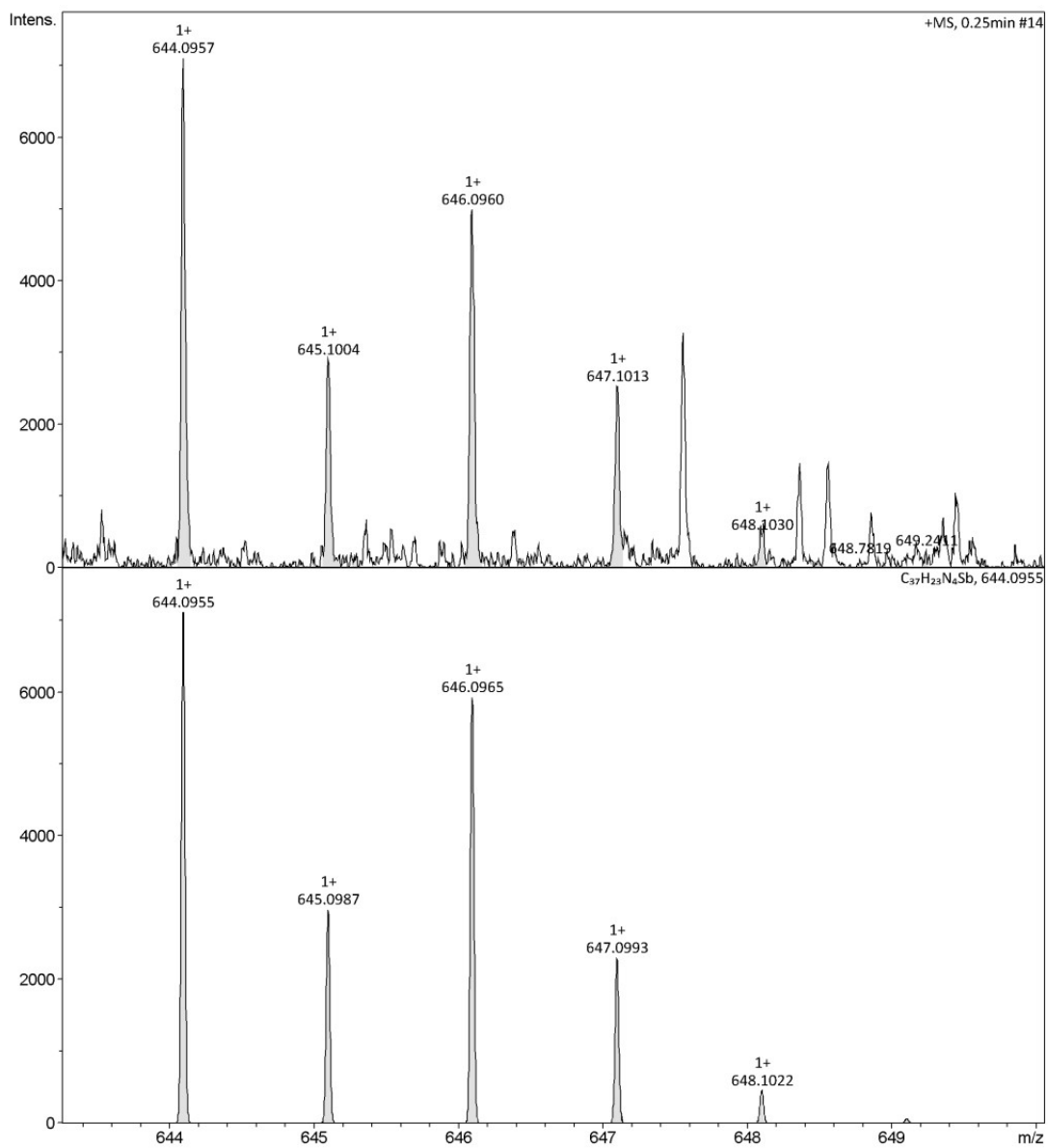


Fig. S23 ESI-HRMS spectrum of  $F_0C-Sb$

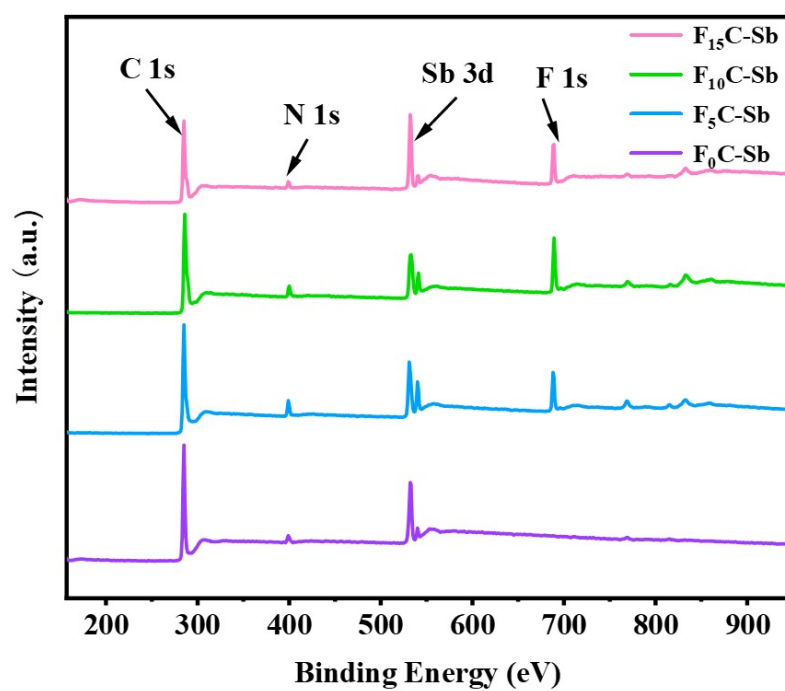


Fig. S24 XPS survey scan spectrum ( $F_{15}C-Sb$  to  $F_0C-Sb$ ).

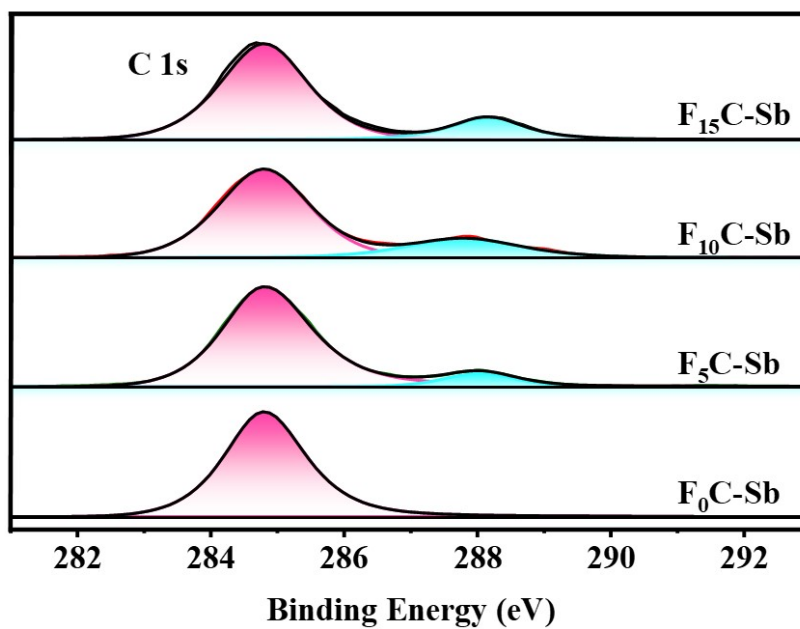


Fig. S25 XPS spectra for C 1s ( $F_{15}C-Sb$  to  $F_0C-Sb$ ).

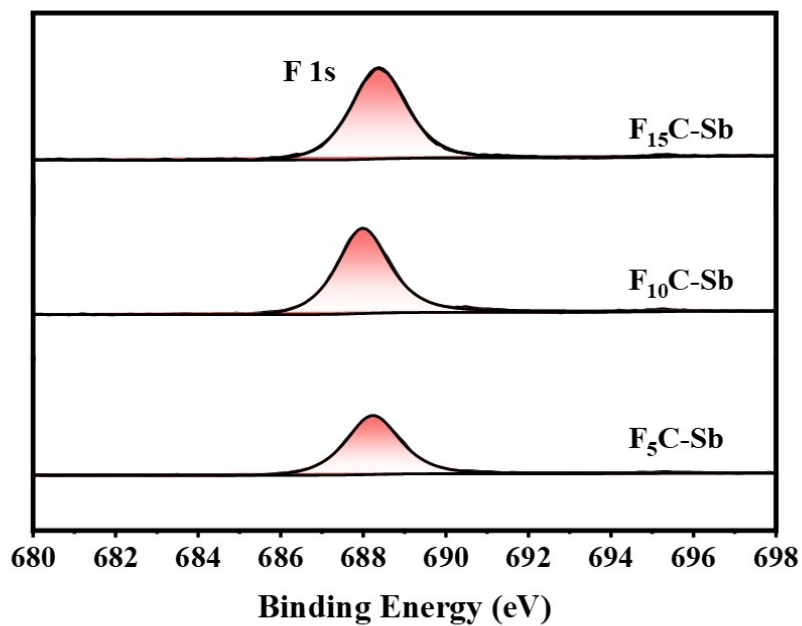


Fig. S26 XPS spectra for F 1s (F<sub>15</sub>C-Sb to F<sub>0</sub>C-Sb).

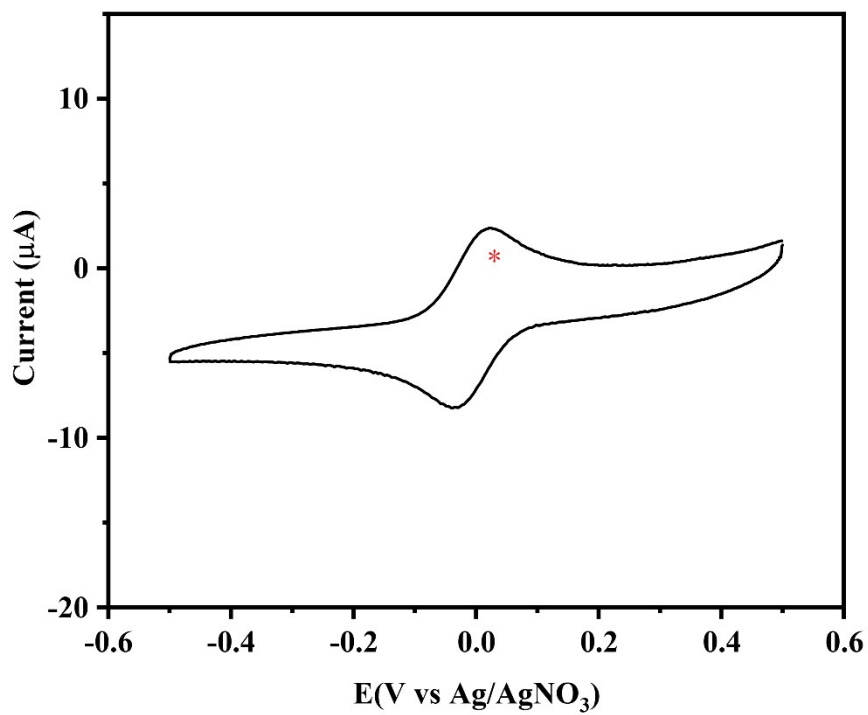


Fig. S27 The redox couple of  $Fc^+/Fc$  in DMF containing 0.1M TBAP with blank glassy carbon

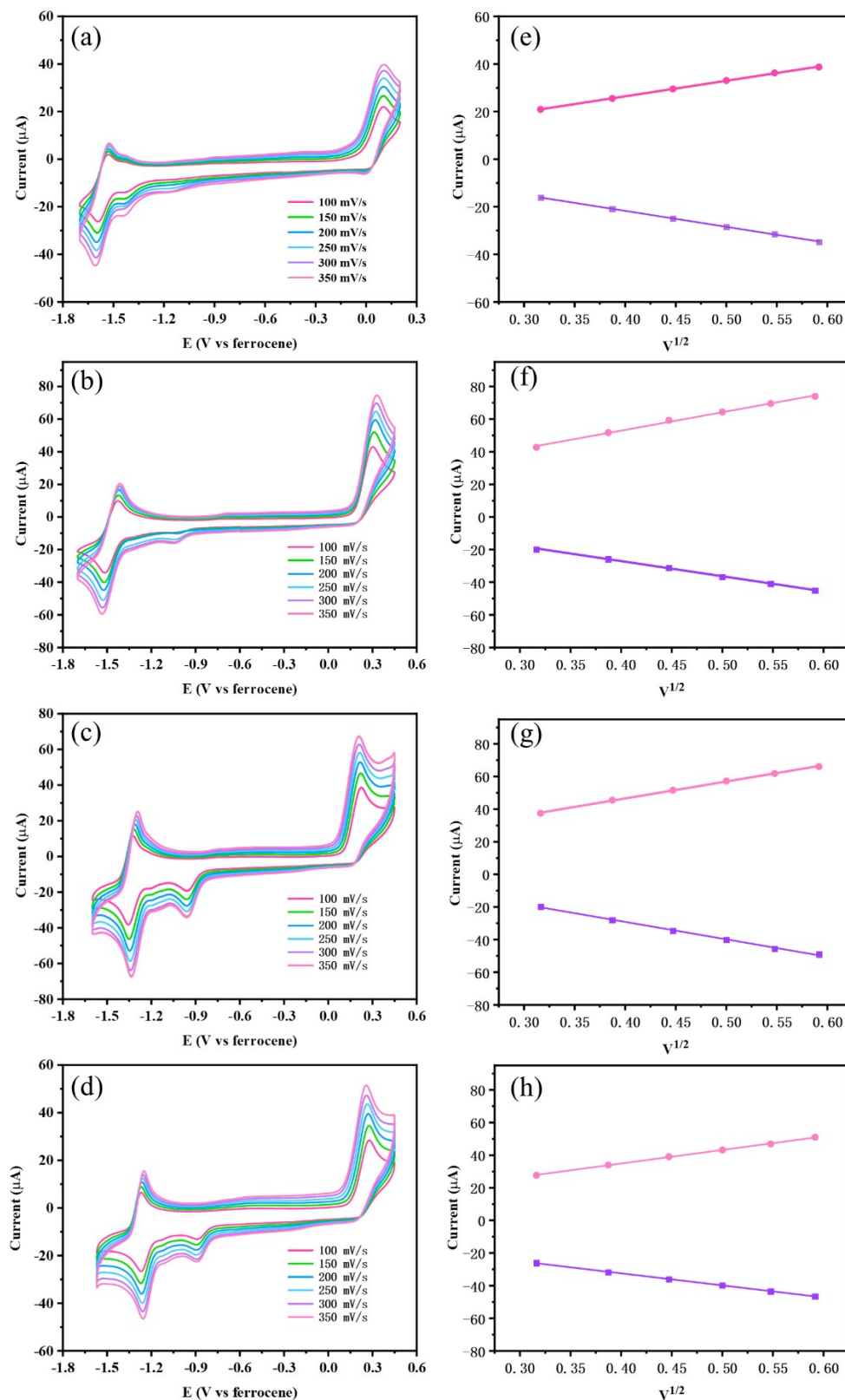


Fig. S28 CVs with a varying scan rate ( $v$ ) from 100 mV/s to 350 mV/s and the maximum current ( $i_p$ ) plots of [Sb-corrole]/[Sb-corrole]<sup>-</sup> reduction and first oxidation waves vs. the scan rate ( $v^{1/2}$ ). (**F<sub>15</sub>C-Sb** (a, e), **F<sub>10</sub>C-Sb** (b, f), **F<sub>5</sub>C-Sb** (c, g) and **F<sub>0</sub>C-Sb** (d, h))

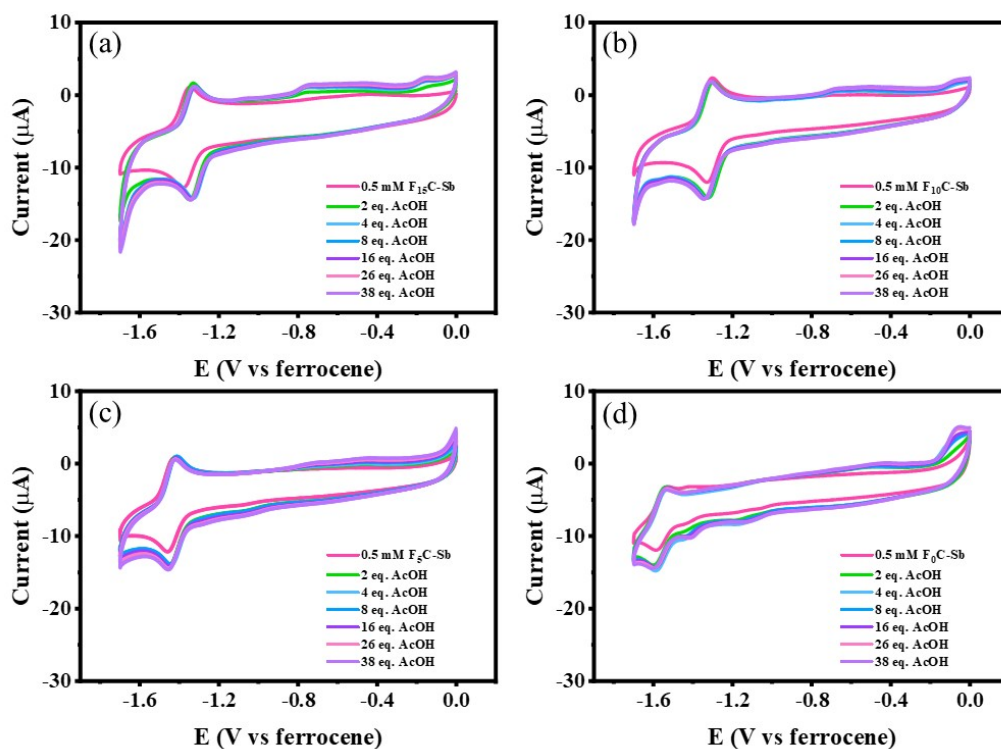


Fig. S29 CVs of 0.5 mM antimony complexes (**F<sub>15</sub>C-Sb** to **F<sub>0</sub>C-Sb**) (a-d) with increasing amounts of AcOH from 0 to 38 equivalents in N<sub>2</sub>-saturated DMF

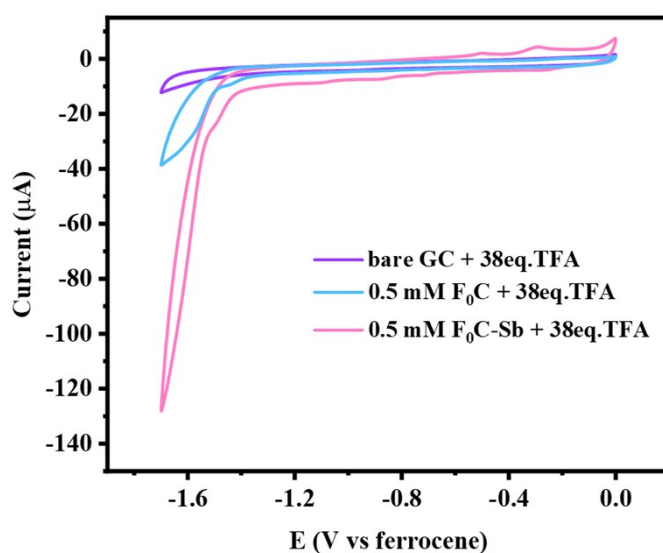


Fig. S30 CVs of bare glassy carbon electrode, 0.5 mM **F<sub>0</sub>C** and 0.5 mM **F<sub>0</sub>C-Sb** in DMF with 38 equivalents TFA



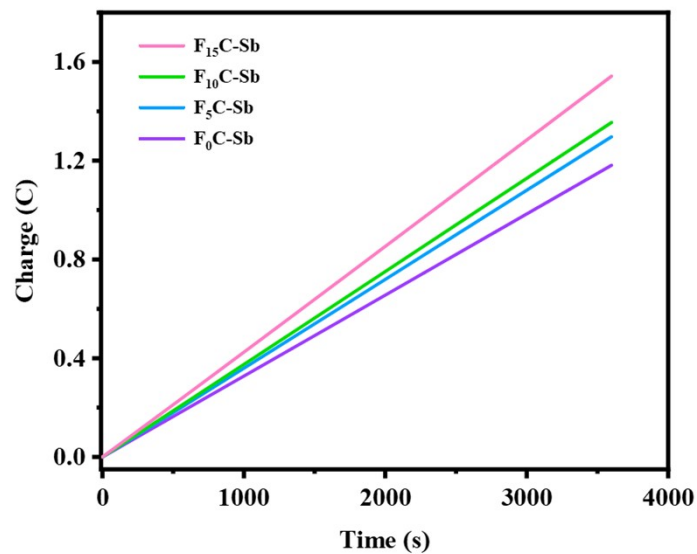


Fig. S31 Charge of 0.5 mM  $F_{15}C-Sb$ ,  $F_{10}C-Sb$ ,  $F_5C-Sb$  and  $F_0C-Sb$  after 1 h of electrolysis in DMF with 38 equivalents TFA

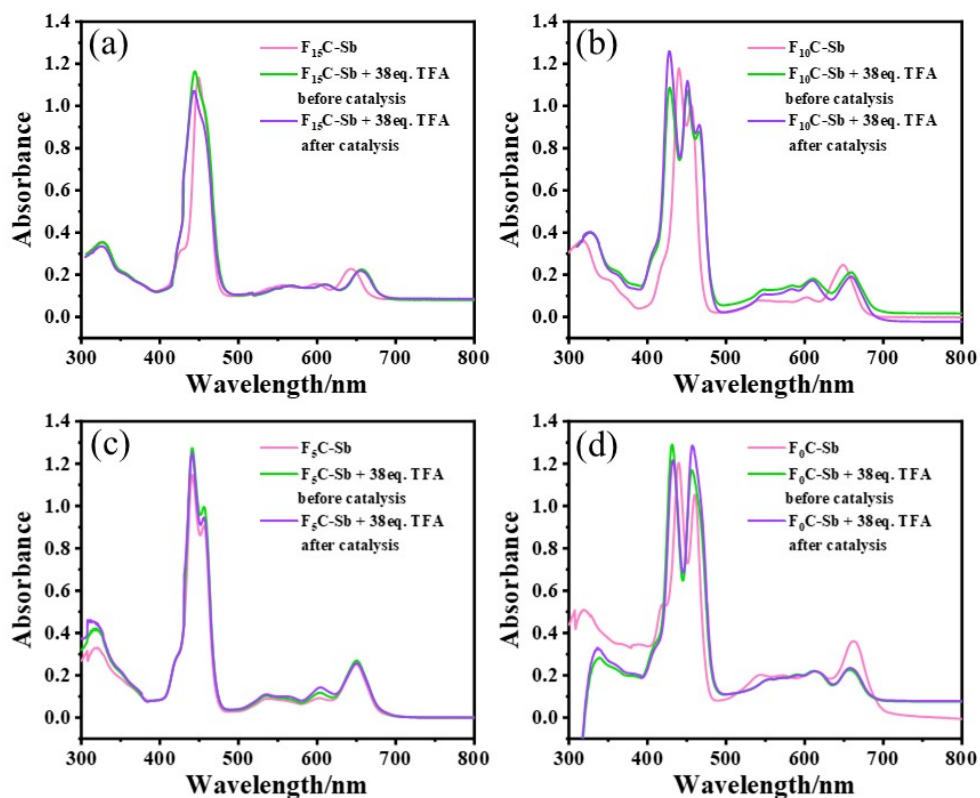


Fig. S32 UV-vis spectra of 0.5 mM  $F_{15}C-Sb$  to  $F_0C-Sb$  in DMF with 38 equivalents TFA and after 1 h electrolysis

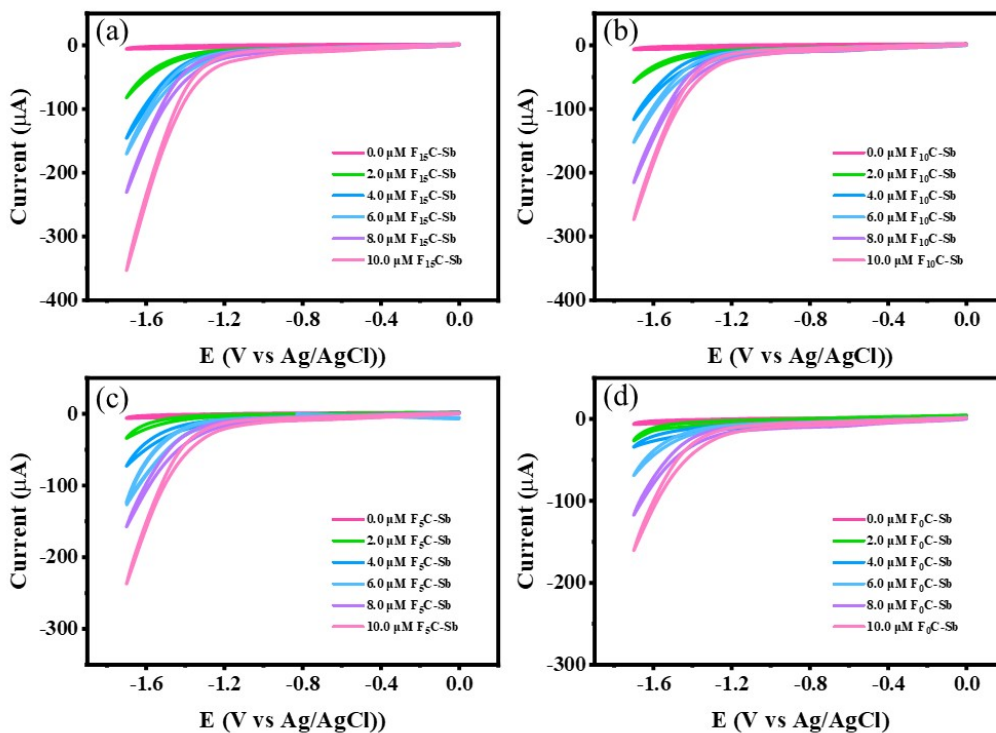


Fig. S33 CVs of various concentrations of  $F_{15}C-Sb$ ,  $F_{10}C-Sb$ ,  $F_5C-Sb$  and  $F_0C-Sb$  (0.0  $\mu M$ –10.0  $\mu M$ ) in buffer solutions at pH=7.0 ( $V_{DMF}/V_{H_2O} = 1/2$ ).

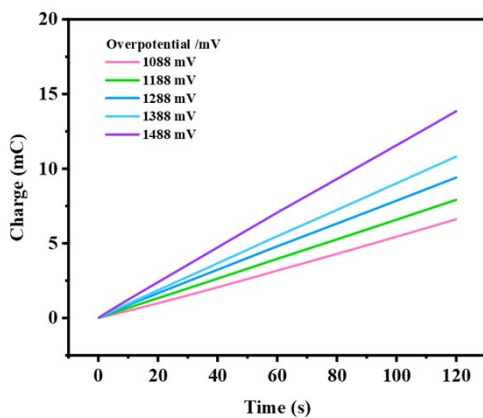


Fig. S34 Charge accumulation of electrolyzing 0.20 M buffer at pH=7.0 without catalyst under different applied potentials (-1.7 V to -2.1 V vs Ag/AgCl) for 2 minutes.

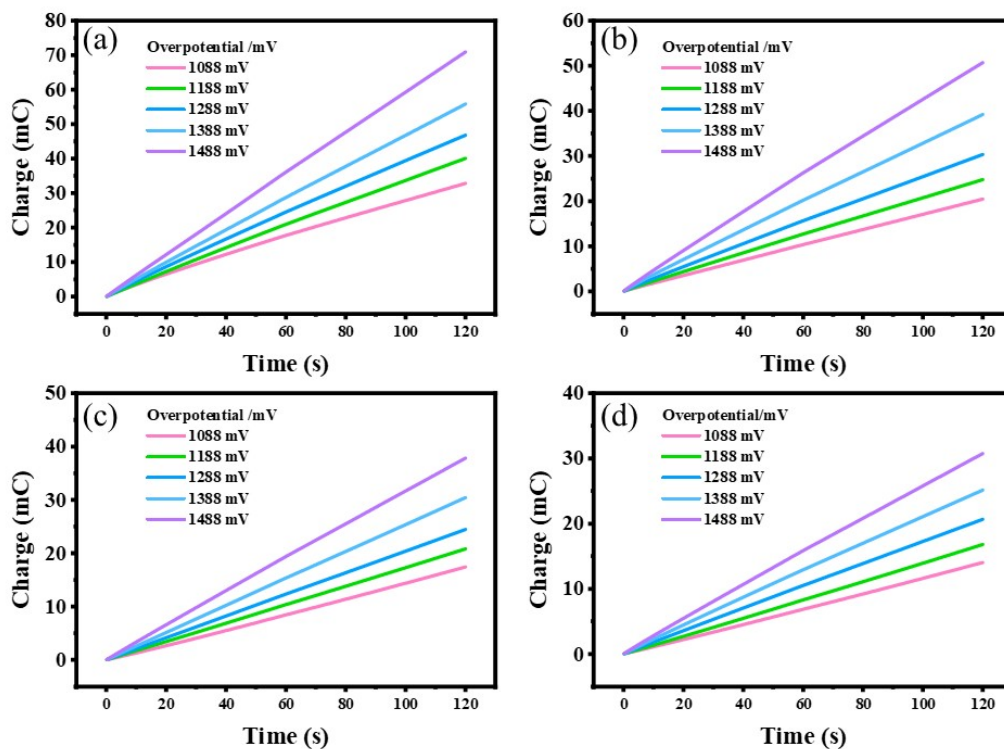


Fig. S35 Charge accumulation of electrolyzing 10  $\mu M$   $F_{15}C-Sb$ ,  $F_{10}C-Sb$ ,  $F_5C-Sb$  and  $F_0C-Sb$  at a range of overpotentials in buffer solutions at pH=7.0 for 2 minutes (a-d).

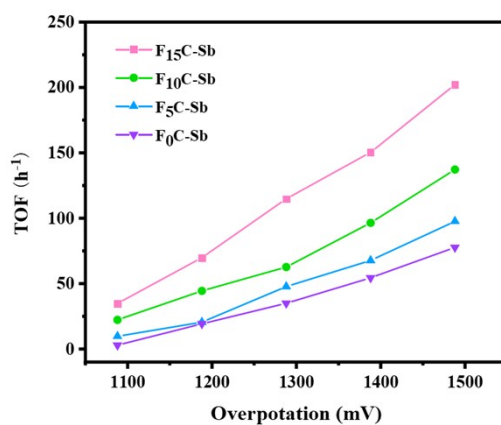


Fig. S36 TOF values of 10  $\mu M$   $F_{15}C-Sb$ ,  $F_{10}C-Sb$ ,  $F_5C-Sb$  and  $F_0C-Sb$  at different overpotentials in buffer solutions at pH=7.0.

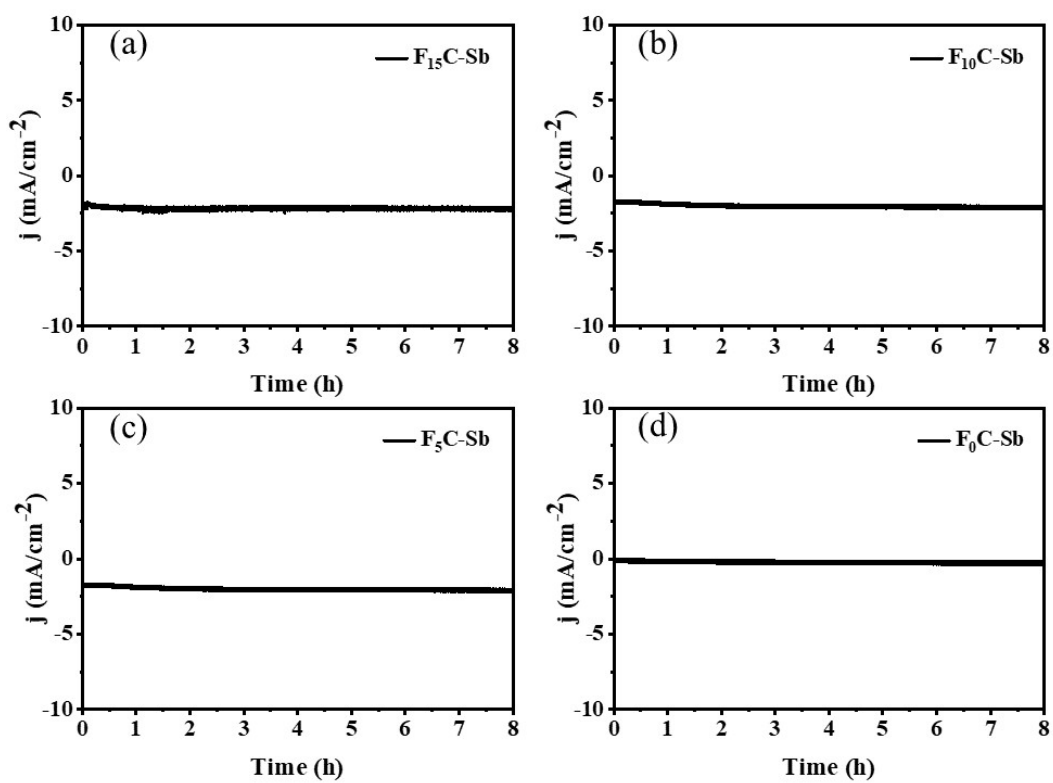


Fig. S37 Current versus 10  $\mu\text{M}$   $\text{F}_{15}\text{C-Sb}$ ,  $\text{F}_{10}\text{C-Sb}$ ,  $\text{F}_5\text{C-Sb}$  and  $\text{F}_0\text{C-Sb}$  in buffer solution at pH = 7.0 at -1.7 V for 8 h electrolysis.

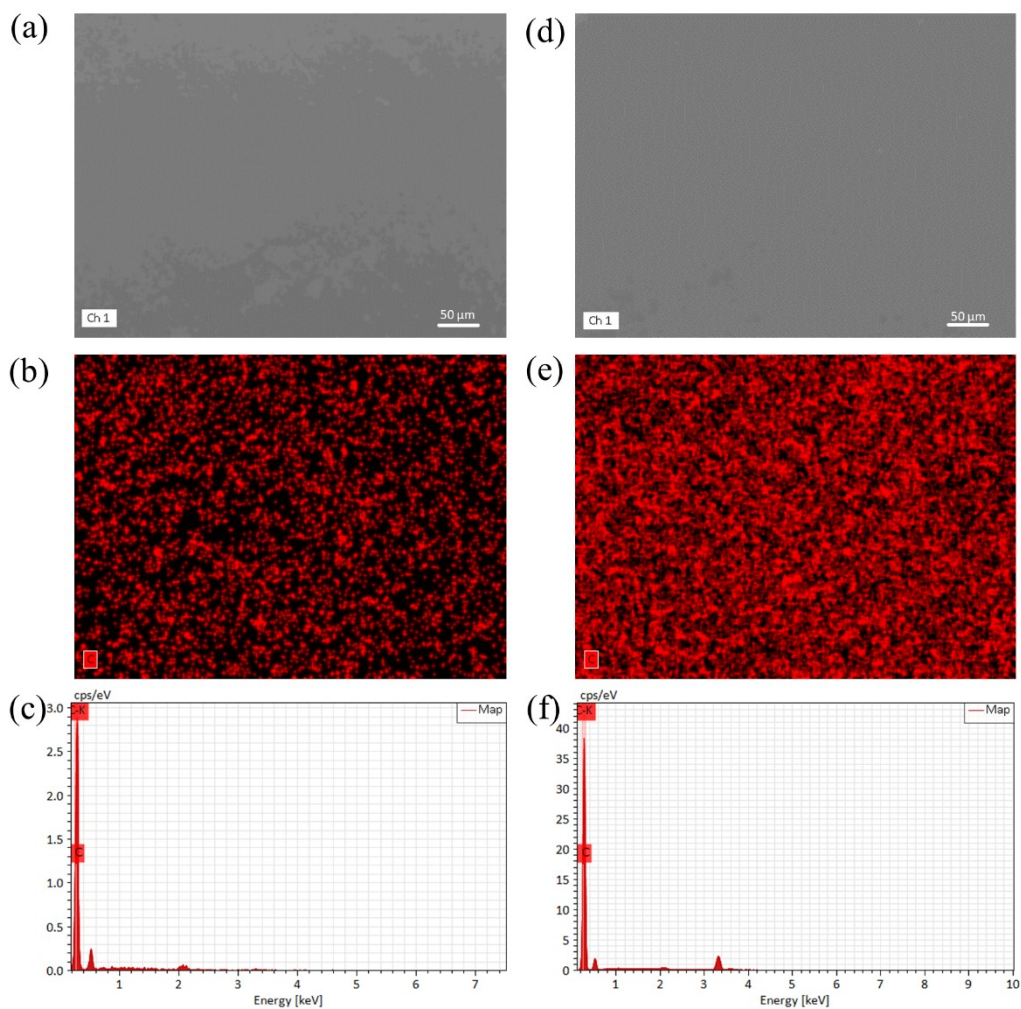


Fig. S38 SEM images and EDX data of GC electrodes before (a-c) and after (d-f) electrolysis.

Complex	Oxidation/V	Reduction/V
	[Sb-corrole]/[Sb-corrole] <sup>+</sup>	[Sb-corrole]/[Sb-corrole] <sup>-</sup>
<b>F<sub>15</sub>C-Sb</b>	0.15	-1.41
<b>F<sub>10</sub>C-Sb</b>	0.16	-1.46
<b>F<sub>5</sub>C-Sb</b>	0.22	-1.50
<b>F<sub>0</sub>C-Sb</b>	0.29	-1.55

Table S1 Redox potentials (V vs ferrocene) of antimony(III) corroles in DMF.

Complex	38 eq. TFA		38 eq. TsOH	
	$i_c/i_p$	TOF ( $s^{-1}$ )	$i_c/i_p$	TOF ( $s^{-1}$ )
<b>F<sub>15</sub>C-Sb</b>	12.61	30.85	14.21	39.17
<b>F<sub>10</sub>C-Sb</b>	11.55	25.88	12.41	29.87
<b>F<sub>5</sub>C-Sb</b>	9.38	17.06	10.84	22.79
<b>F<sub>0</sub>C-Sb</b>	6.90	9.24	9.80	18.63

Table S2 Catalytic activity parameter of four antimony(III) corroles in 38 eq. TFA and TsOH.

Complex	Protonsource	Overpotential (mV)	TOF	Refs.
<b>F<sub>15</sub>C-Sb(III)</b>	19 mM TsOH	770	39.17 $s^{-1}$	This work
<b>F<sub>15</sub>C-Sb(III)</b>	8 mM TFA	770	5.8 $s^{-1}$	This work
<b>F<sub>10</sub>C-Sb(III)</b>	19 mM TFA	770	25.88 $s^{-1}$	This work
<b>F<sub>5</sub>C-Sb(III)</b>	19 mM TFA	790	17.06 $s^{-1}$	This work
<b>F<sub>0</sub>C-Sb(III)</b>	19 mM TFA	820	9.24 $s^{-1}$	This work
<b>F<sub>15</sub>C-P(V)</b>	16 mM TFA	900	9.5 $s^{-1}$	<sup>1</sup>
<b>F<sub>10</sub>C-P(V)</b>	16 mM TFA	900	19.4 $s^{-1}$	<sup>1</sup>
<b>F<sub>5</sub>C-P(V)</b>	16 mM TFA	900	23.5 $s^{-1}$	<sup>1</sup>
<b>F<sub>0</sub>C-P(V)</b>	16 mM TFA	900	721.8 $s^{-1}$	<sup>1</sup>
<b>2-NBPC-Sb(III)</b>	19 mM TFA	642	17.65 $s^{-1}$	<sup>2</sup>
<b>3-NBPC-Sb(III)</b>	19 mM TFA	660	12.48 $s^{-1}$	<sup>2</sup>
<b>4-NBPC-Sb(III)</b>	19 mM TFA	677	11.66 $s^{-1}$	<sup>2</sup>

<b>F<sub>15</sub>C-Sb(III)</b>	10 mM TFA	720	1.86 s <sup>-1</sup>	3
<b>TTC-Sb(III)</b>	20 mM TFA	460	6.72 s <sup>-1</sup>	3
<b>TDOC-Sb(III)</b>	20 mM TFA	1010	2.63 s <sup>-1</sup>	3
<b>(corrolato)(oxo)-Sb(V)</b>	50 mM TFA	420	0.44 h <sup>-1</sup>	4
<b>TPFC (oxo)-Mo(V)</b>	29 mM DMF-H <sup>+</sup>	/	23 s <sup>-1</sup>	5
<b>3-TPFC (oxo)-Mo(V)</b>	29 mM DMF-H <sup>+</sup>	/	2.48 s <sup>-1</sup>	5
<b>3-BPFC-Co(III)</b>	18.26 mM TFA	600	134.56 s <sup>-1</sup>	6
<b>3-BPFC-Co(III)</b>	18.26 mM TsOH	600	62.17 s <sup>-1</sup>	6
<b>F<sub>15</sub>C-Co(III)</b>	5 mM TFA	1010	11 s <sup>-1</sup>	7
<b>TTC-Co(III)</b>	5 mM TFA	1010	17 s <sup>-1</sup>	7
<b>F<sub>15</sub>C-Mn</b>	20 mM TFA	1343	69.34 h <sup>-1</sup>	8
<b>F<sub>10</sub>C-Mn</b>	20 mM TFA	1343	61.74 h <sup>-1</sup>	8
<b>F<sub>10</sub>C-Si</b>	16 mM TFA	1086	15.37 s <sup>-1</sup>	9

Table S3 TOF and overpotential of corrole complexes as electrocatalysts for HER.

#### References:

- 1 G. Yang, Z. Ullah, W. Yang, K. H. Wook, Z. X. Liang, X. Zhan, G. Q. Yuan and H. Y. Liu, *ChemSuschem*, 2023, **16**, e202300211.
- 2 Q.-W. Yan, L.-W. Wu, Z.-W. Liu, F. Chen, C. Ling, H.-Y. Liu, X.-Y. Xiao and L.-P. Si, *Green chemistry*, 2024, **26**, 4574-4581.
- 3 S. Kumar, S. Fite, E. Remigi, A. Mizrahi, N. Fridman, A. Mahammed, T. P. Bender and Z. Gross, *Chem. Eur. J.*, 2024, **30**, e202402145.

- 4 R. Chakraborty, B. Ojha, T. Pain, T. W. Tsega, A. Tarai, N. C. Jana, C.-H. Hung and S. Kar, *Inorg. Chem.*, 2024, **63**, 21462-21473.
- 5 P. Yadav, I. Nigél-Etinger, A. Kumar, A. Mizrahi, A. Mahammed, N. Fridman, S. Lipstman, I. Goldberg and Z. Gross, *iScience*, 2021, **24**, 102924.
- 6 F. Jun-Jia, J. Lan, G. Yang, Y. Gao-Qing, L. Hai-Yang and S. Li-Ping, *New J. Chem.*, 2021, **45**, 5127-5136.
- 7 A. Kumar, S. Fite, A. Raslin, S. Kumar, A. Mizrahi, A. Mahammed and Z. Gross, *Acs Catal*, 2023, **13**, 13344-13353.
- 8 B. Wan, F. Cheng, J. Lan, Y. Zhao, G. Yang, Y.-M. Sun, L.-P. Si and H.-Y. Liu, *Int. J. Hydrogen Energy*, 2023, **48**, 5506-5517.
- 9 Z. W. Liu, G. Yang, S. Y. Xu, W. Y. Xie, Y. F. Yao, X. Y. Xiao, L. P. Si and H. Y. Liu, *Eur. J. Inorg. Chem.*, 2024, **27**, e202300790.